








## RESEARCH ARTICLE

# Ground validation of TRMM 3B43 V7 precipitation estimates over Colombia. Part I: Monthly and seasonal timescales

Sara M. Vallejo-Bernal<sup>1</sup>  | Viviana Urrea<sup>1</sup>  | Juan M. Bedoya-Soto<sup>1</sup>  |  
 Daniela Posada<sup>1</sup>  | Alejandro Olarte<sup>1</sup> | Yadira Cárdenas-Posso<sup>2</sup> |  
 Franklyn Ruiz-Murcia<sup>2</sup> | María T. Martínez<sup>2</sup> | Walter A. Petersen<sup>3</sup>  |  
 George J. Huffman<sup>4</sup>  | Germán Poveda<sup>1</sup> 

<sup>1</sup>Facultad de Minas, Departamento de Geociencias y Medio Ambiente, Universidad Nacional de Colombia, Sede Medellín, Medellín, Colombia

<sup>2</sup>Departamento de Meteorología, Instituto de Hidrología, Meteorología y Estudios Ambientales, IDEAM, Bogotá, Colombia

<sup>3</sup>Science Research and Projects Division, NASA Marshall Space Flight Center, Huntsville, Alabama

<sup>4</sup>Laboratory for Mesoscale Atmospheric Processes, NASA Goddard Space Flight Center, Greenbelt, Maryland

## Correspondence

Germán Poveda, Facultad de Minas, Departamento de Geociencias y Medio Ambiente, Universidad Nacional de Colombia, Sede Medellín, Carrera 80 No 65-223, Bloque M2, Of 315, Medellín, Colombia.

Email: gpoveda@unal.edu.co

## Funding information

HERMES program of Universidad Nacional de Colombia at Medellín, Grant/Award Number: 35973

## Abstract

In this study, we validate precipitation estimates remotely sensed by the Tropical Rainfall Measuring Mission (TRMM) at monthly and seasonal timescales, during the period 1998–2015, by calculating and analyzing diverse error metrics between the 3B43 V7 product and in situ measurements from 1,180 rain gauges over Colombia, of which at least 987 are fully independent of TRMM. We explore the existence of spatiotemporal patterns to assess the performance of 3B43 V7 over the five major natural regions of Colombia: Caribbean, Pacific, Andes, Orinoco and Amazon. The results show that 3B43 V7 product is able to capture the phase of the annual cycle of monthly mean precipitation, but the performance is not good for the amplitude, in particular over the Andes and Pacific regions owing to complex climatic and topographic conditions. In general, 3B43 V7 exhibits good performance in the low-lying and plain Amazon, Orinoco and Caribbean regions. Over the Andes region, characterized by complex topography, overestimation errors are identified [root mean squared error (RMSE)  $\geq 83.59 \text{ mm} \cdot \text{month}^{-1}$  and relative bias (BIAS)  $\geq 4.69\%$ ], whereas the extremely wet rainfall regime of the Pacific region is largely underestimated (RMSE  $\geq 253.52 \text{ mm} \cdot \text{month}^{-1}$  and BIAS  $\leq -11.75\%$ ). These errors are greater during the wet seasons when the metrics reach worse scores than those reported in similar studies worldwide. Occurrence analyses showed that 3B43 V7 misses very frequent light rainfall events and less frequent but very heavy storms, which contribute to the overall underestimation (overestimation) observed over the Andes (Pacific) region. The error characteristics identified and quantified in this study confirm the well-documented limitations of remote precipitation sensing and constitute a warning about major challenges that complex climatic and physiographic features can impose on satellite rainfall missions.

**KEYWORDS**

Colombia, error metrics, ground validation, monthly timescale, precipitation, seasonal timescale, TRMM

## 1 | INTRODUCTION

The understanding of the spatial and temporal variability of precipitation and the accurate quantification of rainfall amounts reaching the land surface are paramount for water resources management, risk assessment, fresh water supply, infrastructure planning, among others. However, rainfall measurements using rain gauges are not fully adequate due to the strong spatiotemporal variability of precipitation, more so of orographic and convective tropical mountain rainfall, which implies the need for frequent and closely spaced observations to correctly represent its structure and behavior (Huffman *et al.*, 2007, 2010). Moreover, such in situ measurements are challenging in many places as remote areas, deserts, forests, high altitudes, over the ocean or in developing countries, where land-based instruments are nonexistent or very scarce or where the access to available data is not possible (Overpeck *et al.*, 2011). This lack of adequate ground-based rainfall estimates limits the understanding of the hydrological cycle and the multiple interconnections between diverse hydroclimatic processes (Condom *et al.*, 2011) and affects the reliability of decision-making models and simulations (Derin *et al.*, 2016).

As an opportunity to overcome these challenges, in the last decades, several satellite missions were designed and launched to observe and measure strategic atmospheric variables from space. Through remote sensing techniques, precipitation fields and time series have been continuously estimated with high spatial and temporal resolution and with quasi-global coverage (Arkin and Ardanuy, 1989; Huffman, 1997; Joyce *et al.*, 2004). Amongst these efforts are two joint missions of the National Aeronautics and Space Administration (NASA) and the Japan Aerospace Exploration Agency. The Tropical Rainfall Measuring Mission (TRMM) and the Global Precipitation Measurement (GPM) mission were both conceived to improve the understanding of the precipitation distribution and variability in the current climate system (Kummerow *et al.*, 1998; Liu *et al.*, 2012; Skofronick-Jackson *et al.*, 2017).

TRMM was a research satellite launched in 1997 with five instruments on board: (a) the precipitation radar (PR) to measure the distribution and intensity of rainfall; (b) the microwave imager to sense the content of the precipitation column and identify rainfall types (e.g. stratiform or convective); (c) the visible and infrared scanner

(VIRS) to provide high-resolution observations on coverage, type and top temperature of clouds (Kummerow *et al.*, 1998); (d) the cloud and the Earth radiant energy sensor to measure the energy at the top and within the atmosphere (Lee *et al.*, 1998) and (e) the lightning imaging sensor to detect and locate lightning with storm-scale resolution (Christian *et al.*, 1992). TRMM gathered climatic data over the tropical and subtropical regions of the Earth for more than 17 years, until it was turned off after fuel depleted in 2015 (Huffman *et al.*, 2007, 2010). Building on the success of TRMM, in 2014 the GPM Core Observatory was launched to unify precipitation measurements from a constellation of research and operational satellites and to improve TRMM-era estimates. GPM carries an advanced radar/radiometer system to extend coverage to higher latitudes and to measure light rain ( $<0.5 \text{ mm}\cdot\text{hr}^{-1}$ ), solid precipitation and the microphysical properties of precipitating particles (Hou *et al.*, 2014).

As a result of the TRMM mission, multiple gridded precipitation products are available at several spatial and temporal resolutions within the global latitude belt  $50^{\circ}\text{N}$ – $50^{\circ}\text{S}$ . These products were generated by TRMM multi-satellite precipitation analysis (TMPA) Version 7 algorithm through the combination of data from passive microwave (PMW) and thermal infrared (IR) sensors. When possible, land surface monthly precipitation gauge analyses developed by the Global Precipitation Climatology Centre (GPCC) were also assimilated (Huffman and Bolvin, 2015). Due to the integration of TRMM and GPM missions, some of these gridded precipitation estimates are running from 1998 to the present (Bolvin and Huffman, 2015; Huffman, 2019).

As expected, numerous studies have used these TMPA products as rainfall estimates to calibrate and implement climatic and hydrological models (Negri *et al.*, 2002; Collischonn *et al.*, 2008; Tapiador *et al.*, 2012; Meng *et al.*, 2014), characterize climatic features (Nesbitt *et al.*, 2000; Petersen and Rutledge, 2001; Biasutti *et al.*, 2012; Mohr *et al.*, 2014; Zuluaga and Houze Jr, 2015; Jaramillo *et al.*, 2017), study extreme events (Zipser *et al.*, 2006; Curtis *et al.*, 2007; Jiang *et al.*, 2011; Rasmussen *et al.*, 2013; Hamada *et al.*, 2014), among others. However, satellite precipitation estimates such as TMPA products have several sources of uncertainty. Individual satellites and their instruments have short life spans over which their orbits and sensitivities are likely

to change. Also, the use of advanced data-processing techniques is required and the resulting data should be reprocessed as previously unknown problems are discovered (Overpeck *et al.*, 2011). The intrinsic difficulties and the intensive use of these satellite products made evident the need to quantify the uncertainty in the precipitation estimates, and multiple validation studies have been conducted for the TMPA algorithm.

On a global scale, different continental regimes have been evaluated (Ebert *et al.*, 2007; Tian and Peters-Lidard, 2010; Stampoulis and Anagnostou, 2012; Maggioni *et al.*, 2016). Also, more specialized regional assessments have been conducted over each continental regime: North America (Tian *et al.*, 2009; Gourley *et al.*, 2010; Sapiano *et al.*, 2010; Chen *et al.*, 2013b), South America (Su *et al.*, 2008; Scheel *et al.*, 2011; Ochoa *et al.*, 2014; Zulkafli *et al.*, 2014; Melo *et al.*, 2015; Zambrano-Bigiarini *et al.*, 2017), Europe (Kidd *et al.*, 2012; Derin and Yilmaz, 2014; Duan *et al.*, 2016; Nastos *et al.*, 2016), Africa (Adeyewa and Nakamura, 2003; Nicholson *et al.*, 2003; Hirpa *et al.*, 2010; Dinku *et al.*, 2011), and Asia (Nair *et al.*, 2009; Yong *et al.*, 2010; Krakauer *et al.*, 2013; Chen *et al.*, 2013a). For a detailed review of satellite precipitation products accuracy during the TRMM era, see Maggioni *et al.* (2016) and references therein. All these validation studies have confirmed that the performance of TMPA rainfall estimates is strongly dependent on the climate regime and the topographic features of the study region. Then, the need for a comprehensive evaluation of satellite precipitation data sets on a regional basis instead of using global approaches has been remarked. Also, calibration-validation data sets that are representative of diverse climate regimes around the globe are needed for a plethora of applications (Huffman, 1997; Huffman *et al.*, 1997; Kummerow *et al.*, 2000). Validation efforts across different regions with complex topographic or climatic features would lead to developing error correction procedures to globally improve these estimates (Derin *et al.*, 2016). However, most of the studies over regions with those specific features have evaluated TMPA products against reanalysis data (Ward *et al.*, 2011), scarce land-based observations (Hirpa *et al.*, 2010; Condom *et al.*, 2011; Mantas *et al.*, 2015) or during short periods (Franchito *et al.*, 2009; Gourley *et al.*, 2010).

Colombia, a country located in northwestern South America, exhibits such two challenging characteristics and, thus, provides a paradigmatic case study for the performance of satellite products. Precipitation in Colombia is the result of complex interactions between the dynamics of the Intertropical Convergence Zone (ITCZ), diverse low-level jets, the Caribbean Sea, the Pacific and Atlantic Oceans, the Amazon and Orinoco River basins, land-

atmosphere interactions and precipitation recycling (Bedoya-Soto *et al.*, 2019), and the topography of the Andes (Poveda, 2004; Poveda *et al.*, 2006; Álvarez-Villa *et al.*, 2011). As a consequence climate is very diverse, ranging from an extremely wet precipitation regime in the tropical rainforest of the Pacific coast (Poveda and Mesa, 2000) to a dry regime in the northern desert region of the country (Dinku *et al.*, 2010b).

This is the first of a series of papers aimed at validating rainfall estimates, remotely sensed by TRMM, using in situ measurements over Colombia at multiple time-scales. In particular, the present one evaluates TRMM 3B43 V7 (henceforth 3B43 V7) precipitation product at monthly and seasonal timescales using a large data set of land-based observations over more than 1,100 rain gauges. To that aim, we evaluate the 3B43 V7 product using as ground truth in situ measurements of monthly precipitation gathered by Instituto de Hidrología, Meteorología y Estudios Ambientales (IDEAM), the hydrological and meteorological service of Colombia. We perform the validation at monthly and seasonal time-scales during the period spanning from 1998 to 2015, corresponding to the complete years available for both databases. Given the identified need for challenging validation scenarios, the exceptional climatological and topographic features of Colombia, and the dense data set used as a reference, this study is one of a kind. Through these analyses, our purpose is to characterize the spatiotemporal distribution of errors and to identify the relative roles of climatic and landscape factors influencing the performance of the satellite product over the five major natural regions of the country. Toward those ends, we organize this document as follows: in Section 2 we describe the databases we use and in Section 3 we present the methods we employ to perform the ground validation. Section 4 presents the results, which are discussed in Section 5. Finally, Section 6 presents a summary of our work and draws the conclusions.

## 2 | STUDY AREA AND DATA

### 2.1 | Study area

Colombia is located in the western corner of tropical South America, with coasts on both the Caribbean Sea and the Pacific Ocean, with 40% of its territory within the Amazon River basin, and crossed by the Andes, which are divided into the Western, Central and Eastern mountain ranges (see Figure 1). This branching of the Andes generates complex mountain topography that together with the tropical climate and high rainfall rates produce a lot of ecosystems and microclimates, ranging from

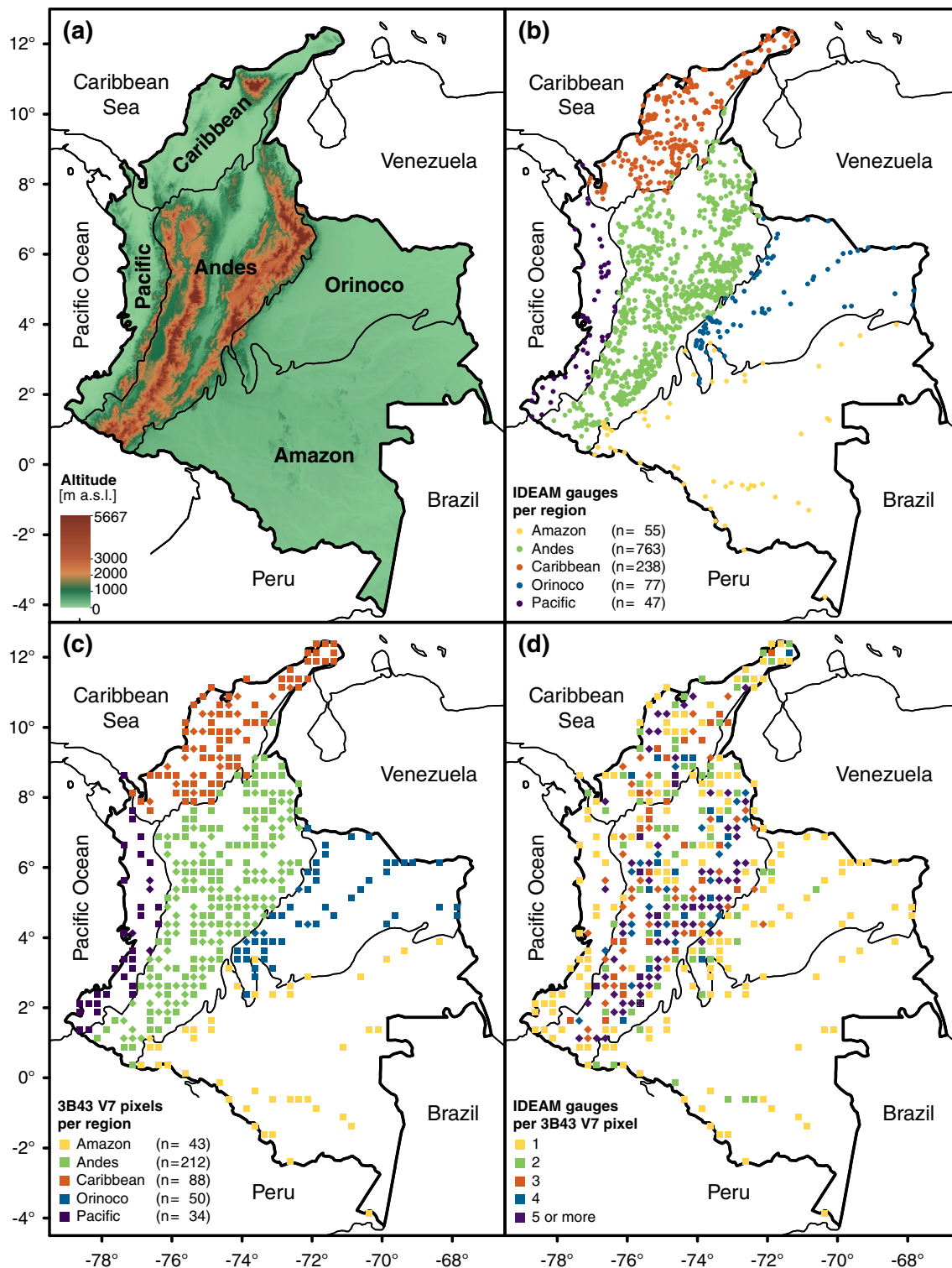


**FIGURE 1** (a) Geographical location and topographical features of the five major natural regions of Colombia: Caribbean, Pacific, Andes, Orinoco and Amazon. Spatial distribution of (b) the 1,180 IDEAM rain gauges, and (c) the 427 3B43 V7 pixels, used for ground-validation. (d) Density map of IDEAM rain gauges available at each 3B43 V7 pixel. The pixels marked with diamonds in panels (c,d) are those with assimilated IDEAM rain gauges [Colour figure can be viewed at [wileyonlinelibrary.com](http://wileyonlinelibrary.com)]

deserts to snowy peaks within a territory of a little more than 1,141,000 km<sup>2</sup>. Because of this, Colombia is divided into five major natural regions, as defined by Instituto

Geográfico Agustín Codazzi: Caribbean, Pacific, Andes, Orinoco and Amazon (Figure 1a). Precipitation in Colombia is the result of the dynamics of macroscale and



mesoscale climatic phenomena, such as the ITCZ and three low-level jets, taking place over a country with about 72% of its territory within the Amazon and Orinoco River basins, crossed by the Andes and surrounded by the Caribbean Sea and the Atlantic ocean. All these climatic drivers interact in complex ways resulting in a diverse climate varying from an extremely wet precipitation regime in the tropical rainforest of the Pacific coast (Poveda and Mesa, 2000) to a dry regime in the northern desert region of the country (Dinku *et al.*, 2010b). Due to the drastic changes in the physical and climatic conditions in exceptionally small distances, Colombia is a challenging region to test for the skill of precipitation measurement missions such as TRMM.

## 2.2 | TRMM 3B43 V7 data

The 3B43 V7 satellite product is a monthly, gauge-adjusted, post-real-time research version product estimated with the TMPA Version 7 algorithm. 3B43 V7 is computed using precipitation-related PMW data, window-channel IR data and a monthly, 1° scale gauge analysis from GPCP. From 1998 to 2010, the Full Data Monthly Product Version 6 (henceforth FDMP V6) is assimilated (Becker *et al.*, 2011), thereafter it is replaced by the Monitoring Analysis Version 4 (henceforth MA V4) (Schneider *et al.*, 2011). First, the original 3-hr remotely sensed IR and microwave estimates are added for the calendar month. Then, the GPCP monthly precipitation gauge analysis is used to create a large-scale bias adjustment to the satellite-only estimates. Finally, the resulting monthly gauge-adjusted satellite-only estimate is combined directly with the precipitation original gauge analysis using inverse error variance weighting (Huffman and Bolvin, 2015). The result is a monthly gridded data set which covers a global belt extending from 50°S to 50°N latitude, at 0.25° spatial resolution (Huffman *et al.*, 2010). For our purposes, 3B43 V7 was downloaded in raster format over the region with latitudes from 5°S to 13°N and longitudes from 80°W to 66°W, spanning the validation period from January 1998 to December 2015. Each layer of the raster files contained the mean hourly rainfall of a month, therefore we multiplied by the number of hours of the respective month to obtain the monthly precipitation. 3B43 V7 has no missing records.

## 2.3 | Rain gauge data

Originally, IDEAM provided information from 2,683 rain gauges in Colombia with monthly precipitation records from 1930 to 2015. From this database, we

initially selected 1,655 rain gauges, those with 30% or less of missing records during the 1998–2015 validation period. Missing monthly records were reconstructed using an algorithm that combines singular value decomposition (SVD) with convex optimization (Kurucz *et al.*, 2007; Candès and Recht, 2009). For validation purposes, we identified 629 pixels from 3B43 V7 containing at least one rain gauge from IDEAM. In the case of having two or more rain gauges within a TRMM pixel, the respective precipitation time series were averaged and used as the ground truth, as practiced by many previous studies (Nicholson *et al.*, 2003; Yong *et al.*, 2010; Scheel *et al.*, 2011; Mantas *et al.*, 2015).

Having in mind that the major GPCP land-based data source over Colombia during our validation period is the meteorological national service (Becker *et al.*, 2013) and that GPCP gauge analysis is assimilated by TMPA at monthly timescale, it is necessary to guarantee the independence between IDEAM stations and 3B43 V7 estimates. To that end, we used Version 8 of FDMP which is available at 0.25° resolution, the same of 3B43 V7, and provides the number of assimilated stations per pixel for each month from 1998 to 2015 (Schneider *et al.*, 2018). Since the number of assimilated stations in FDMP V8 is always greater than both FDMP V6 and MA V4, we can reasonably assume that the number of rain gauges per pixel used to bias-correct 3B43 V7 was, at most, the same as that reported in FDMP V8. Also, the sum of the number of stations per pixel reported by FDMP V8 at 0.25° resolution coincides with the total reported by FDMP V8 at 1°, therefore, it is very likely that if a pixel did not assimilate stations in FDMP V8 at 0.25° scale, it did not assimilate them either in the 1° gauge analysis used to bias-correct 3B43 V7.

Based on these considerations, we used FDMP V8 to choose 427 validation pixels containing 1,180 rain gauges, of which a maximum of 193 were potentially used for bias-correct 3B43 V7. We selected 292 pixels with no assimilated data during every month of 1998–2015, the additional 135 pixels are the ones where the maximum number of assimilated rain gauges in any month is less than half of the stations available in IDEAM data set. These last pixels are not completely independent of 3B43 V7 and can cause the validation to be biased towards better performance than the actual one. However we decided to include them in the analysis for two fundamental reasons: (a) strict inequality guarantees that IDEAM mean time series associated to the pixel is dominated by non-assimilated rain gauges, and (b) these pixels are an opportunity to verify if the bias correction really improves the performance of TMPA products in neighboring stations that

were not assimilated in GPCC gauge analysis. Figure 1b,c shows the spatial distribution of the 1,180 rain gauges and the 427 pixels within the five major natural regions of Colombia, with the sample size indicated on the bottom left margin of the panel. Figure 1d shows the number of rain gauges used to calculate IDEAM mean time series of each pixel.

### 3 | METHODS

We assess the performance of 3B43 V7 using as ground truth IDEAM's monthly rainfall measurements, on a pixel-by-pixel basis over Colombia, at monthly and seasonal timescales, during the period spanning from 1998 to 2015, corresponding to the complete years available for both databases. Seasonal analyses of this study are based on the climatological seasons in Colombia: June, July and August (JJA); September, October and November (SON); December, January and February (DJF) and March, April and May (MAM), defined by the drier (DJF and JJA) and wetter (MAM and SON) periods of the year over the Andes region.

To decide whether to focus our efforts on ground validating when it rains or how much it rains, we first validate the phase, the amplitude and the cumulative mass curve of the annual cycle of mean precipitation at monthly resolution. Then, we quantify the discrepancies between 3B43 V7 and IDEAM at seasonal timescale in terms of several error metrics (Table 1) and evaluate the existence of spatiotemporal patterns related to the physical aspects that modulate the hydroclimatology of each of

the five major natural regions of the country. We perform a Kolmogorov–Smirnov (KS) test for the null hypothesis that the seasonal precipitation time series of IDEAM and TRMM 3B43 are from the same empirical distribution function and we calculate the KS test rejection rate (KSRR). We use the Spearman rank correlation coefficient ( $\rho$ ) to evaluate the monotonic association (whether linear or not) between satellite precipitation and gauge observations. With the mean error (ME) we estimate the bias in the mean precipitation of both data sets. The mean absolute error (MAE) and the root mean squared error (RMSE) are used to measure the average magnitude of the errors, with the difference that RMSE gives greater weight to the larger errors relative to MAE. Finally, with the relative bias (BIAS) we scale the mean error with respect to the mean precipitation of the gauge observations. Since ME and BIAS are signed, positive (negative) values of these metrics are associated with overestimation (underestimation) of 3B43 V7 with respect to IDEAM. We also validate the capability of 3B43 V7 to detect different rainfall rates by calculating the probability density functions (PDFs) by occurrence with  $50 \text{ mm}\cdot\text{month}^{-1}$  intervals.

### 4 | RESULTS

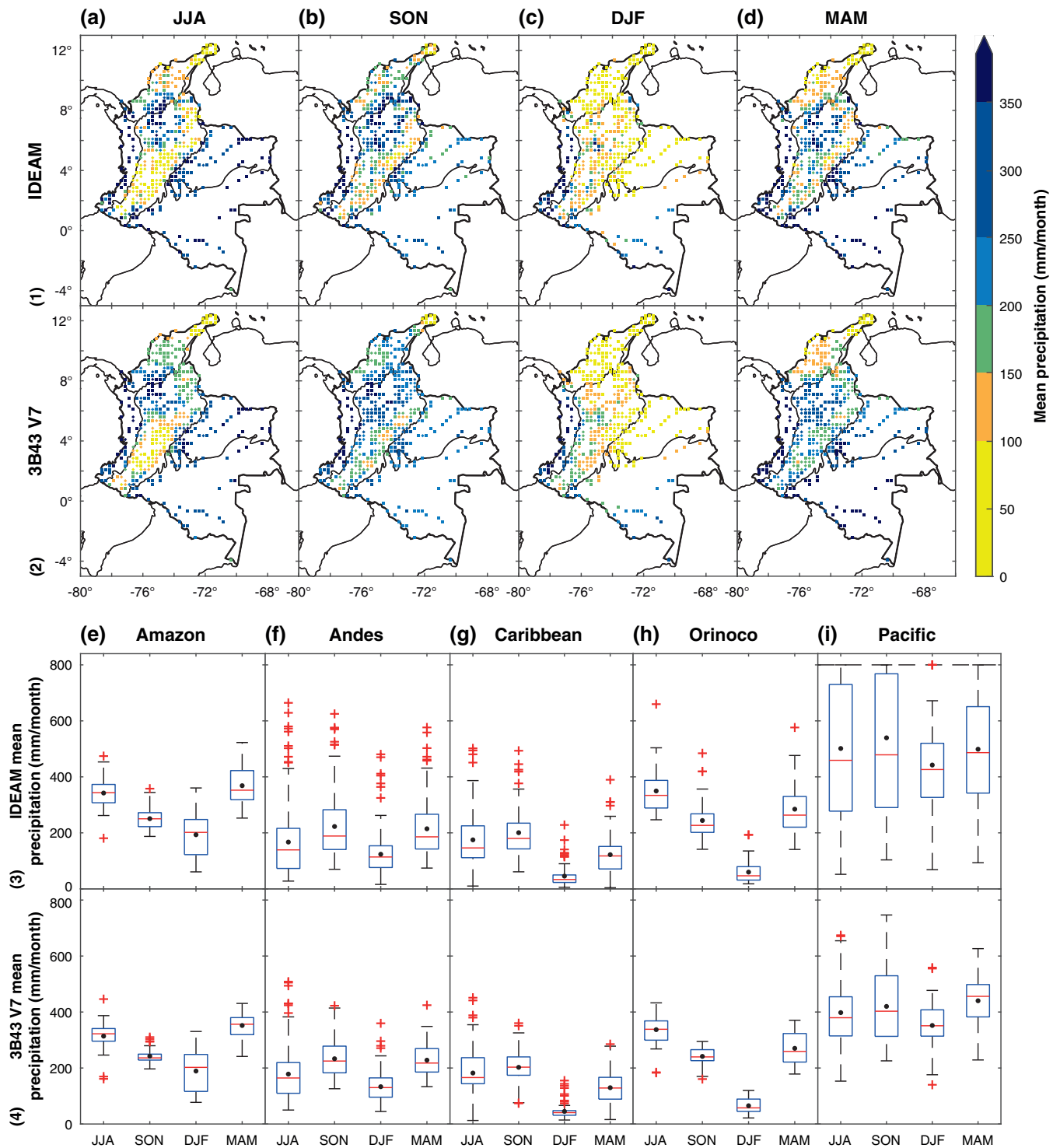
#### 4.1 | The annual cycle of mean precipitation

Figure 2 shows 18-year mean monthly precipitation for each season as seen by IDEAM and 3B43 V7 as well as the corresponding box plots. There are notable

**TABLE 1** Error metrics used to validate the 3B43 V7 satellite product with respect to the in situ measurements of monthly mean precipitation over Colombia

Metric	Units	Expression	Range	Perfect score
KSRR	%	$\text{KSRR} = \frac{\text{Rejected pixels}}{\text{Validated pixels}} \times 100$	[0, 100]	0
Spearman rank correlation ( $\rho$ )	Dimensionless	$\rho = \frac{\text{cov}(r_S, r_G)}{\sigma_{r_S} \sigma_{r_G}}$	[-1, 1]	1
RMSE	$\text{mm}\cdot\text{month}^{-1}$	$\text{RMSE} = \sqrt{\frac{1}{n} \sum_{i=1}^n (S_i - G_i)^2}$	[0, $+\infty$ )	0
ME	$\text{mm}\cdot\text{month}^{-1}$	$\text{ME} = \frac{1}{n} \sum_{i=1}^n (S_i - G_i)$	$(-\infty, +\infty)$	0
MAE	$\text{mm}\cdot\text{month}^{-1}$	$\text{MAE} = \frac{1}{n} \sum_{i=1}^n  S_i - G_i $	[0, $+\infty$ )	0
BIAS	%	$\text{BIAS} = \frac{\sum_{i=1}^n (S_i - G_i)}{\sum_{i=1}^n (G_i)} \times 100$	[-100, $+\infty$ )	0

Note:  $G_i$ , gauged observation (e.g. IDEAM);  $n$ , number of samples;  $r_G$ , rank variable of the gauge observation;  $r_S$ , rank variable of the satellite precipitation;  $S_i$ , satellite estimation (e.g. 3B43 V7);  $\sigma_{r_S}$  and  $\sigma_{r_G}$ , SDs of the rank variables.



**FIGURE 2** Seasonal evaluation of 18-year mean monthly rainfall of IDEAM and 3B43 V7 over the validation pixels in the five major natural regions of Colombia. (a–d) Spatial distribution of precipitation estimates and (e–i) regional box plots. The pixels marked with diamonds in panels (a–d) are those with assimilated IDEAM rain gauges. Dashed horizontal line in panel (i) sets the limit for data display, so that larger values are displayed on it [Colour figure can be viewed at [wileyonlinelibrary.com](http://wileyonlinelibrary.com)]

differences between the regions, not only in the rainfall rates but also in the seasonality of the annual cycle. The Pacific region is the rainiest of the country and arguably of the world (Poveda and Mesa, 2000; Yepes *et al.*, 2019), with pixels reporting monthly mean precipitation rates of

more than  $800 \text{ mm month}^{-1}$ . It is followed by the Amazon and Orinoco regions albeit with significantly lower rainfall amounts. The Caribbean and Andes regions are the driest (Álvarez-Villa *et al.*, 2011). It is also remarkable that the Andes, Caribbean and Pacific regions exhibit a

bimodal annual cycle, with wet (dry) seasons in MAM and SON (JJA and DJF), while the Orinoco and Amazon regions exhibit unimodal annual cycles with a single dry season during DJF (Figure 2e–i). These spatiotemporal patterns can be explained by the meridional migration of the ITCZ which has been identified as the main modulating mechanism of intra-annual variability over Colombia (Poveda, 2004; Poveda *et al.*, 2006), but also by the dynamics of diverse large-scale phenomena that influence the moisture transport and precipitation regime of each region, mainly the three low-level jets present in the country: (a) the Caribbean Low-Level Jet (CLLJ) (Amador, 1998, 2008; Amador and Magana, 1999; Wang, 2007), which is active from northern South America to the Greater Antilles; (b) the Chocó Low-Level Jet (Choco Jet) acting over the far eastern Pacific (Poveda and Mesa, 1999, 2000; Rueda and Poveda, 2006; Sakamoto *et al.*, 2011; Poveda *et al.*, 2014; Bedoya-Soto *et al.*, 2019; Yepes *et al.*, 2019) and (c) the Corriente de los Andes Orientales (CAO) Low-Level Jet or Eastern Andes Low-Level Jet (Montoya *et al.*, 2001; Torrealba and Amador, 2010; Bedoya-Soto *et al.*, 2019), also recently identified as Orinoco Low-Level Jet (Jiménez-Sánchez *et al.*, 2019), which constitutes the northernmost leg of the South American Low-Level Jet (Berbery and Collini, 2000; Marengo *et al.*, 2004; Vera *et al.*, 2006). These mechanisms, together with complex soil–atmosphere interactions over the Andes and the Amazon and Orinoco River basins, contribute to the regional particularities that are evidenced in Figure 2 (Mejía *et al.*, 1999; Poveda, 2004). Despite the differences, it is worth noting that DJF is the driest season all over the country, which can be explained by the southern migration of the ITCZ and the weakening of the Choco Jet.

The variability of the precipitation regime over the major natural regions of Colombia can be examined on a pixel-by-pixel basis. Figure 3 presents the superposition of 18-year mean annual cycles of rainfall intensities and cumulative mass curves at monthly resolution, from June to June according to the hydrological year in Colombia, estimated using IDEAM and 3B43 V7 databases. Panels (a) to (z) show the results for 24 representative validation pixels, selected proportionally to the density of rain gauges of each natural region of the country.

Regarding when it rains, it is worth noting that 3B43 V7 is able to capture, equally precise, the phase of both the unimodal and bimodal annual cycles of mean precipitation at monthly resolution that coexist all over Colombia (Poveda *et al.*, 2006; Urrea *et al.*, 2019), not only on the pixels shown in Figure 3 but on the 427 validation pixels (not shown). This capability seems to be unaffected by the particularities of each region such as topography, climate, land cover and vegetation, among others. The

outstanding performance of 3B43 V7 concerning these temporal patterns was expected, considering the large land-based data set assimilated by 3B43 V7 over Colombia during the period 2001–2005 (Becker *et al.*, 2013), but also because the inter-annual variability of the annual cycle is reflected into changes in its amplitude but not in its phase (Poveda *et al.*, 2001, 2011). For these reasons, from here onwards, we only validate the rainfall rates.

In terms of how much it rains, from Figure 3 it is evident that the mountain topography is a challenging feature for the performance of 3B43 V7 over Colombia when capturing the amplitude of the annual cycle of mean precipitation. It can be noticed that in the Orinoco and Amazon, low-lying and mostly plain regions, 3B43 V7 estimates coincide, almost exactly, with in situ measurements. As an example, Figure 3l,n,p,s,t,v,z shows that the satellite product manages to capture both the average intensity of each month and the amount of rainfall accumulated during the hydrological year. On the contrary, over the Andes and the Caribbean regions, the spatial behavior seems to be correlated with the altitude of the pixel. Both overestimation and underestimation errors are present, but the discrepancies are larger at the highest altitudes (Figure 3j,o,q,w) and tend to decrease (Figure 3b,d,h) reaching a good performance in the inter-Andean valley (Figure 3c,g).

## 4.2 | Spatial and temporal patterns of the metrics' scores

The spatial distribution of errors of 3B43 V7 provides information about its performance dependence on specific physical and geographical features. Figures 4 show maps of the error metrics of 3B43 V7 against IDEAM over Colombia. According to these results, in the Caribbean, Orinoco and Andes (Amazon and Pacific) regions, there is a predominance of seasonal overestimation (underestimation) errors. Specifically, there are underestimation errors in the rainiest areas of the country, those with more than 3,000 mm of rainfall per year (Poveda *et al.*, 2007; Álvarez-Villa *et al.*, 2011) such as the south-eastern part of the Amazon region, the eastern piedmont of the Eastern Andes, the Pacific region and the Mompox depression region located between the Central Caribbean and the Northern Andes regions. Conversely, overestimation errors are found in the driest places of the country, with annual average rainfall between 300 and 1,500 mm, like the mountain tops of the Western and the Eastern Andes and most of the Caribbean region. However, not only the precipitation regime dominates the spatial patterns of the studied metrics, but the mountain topography also constitutes a great challenge for remote



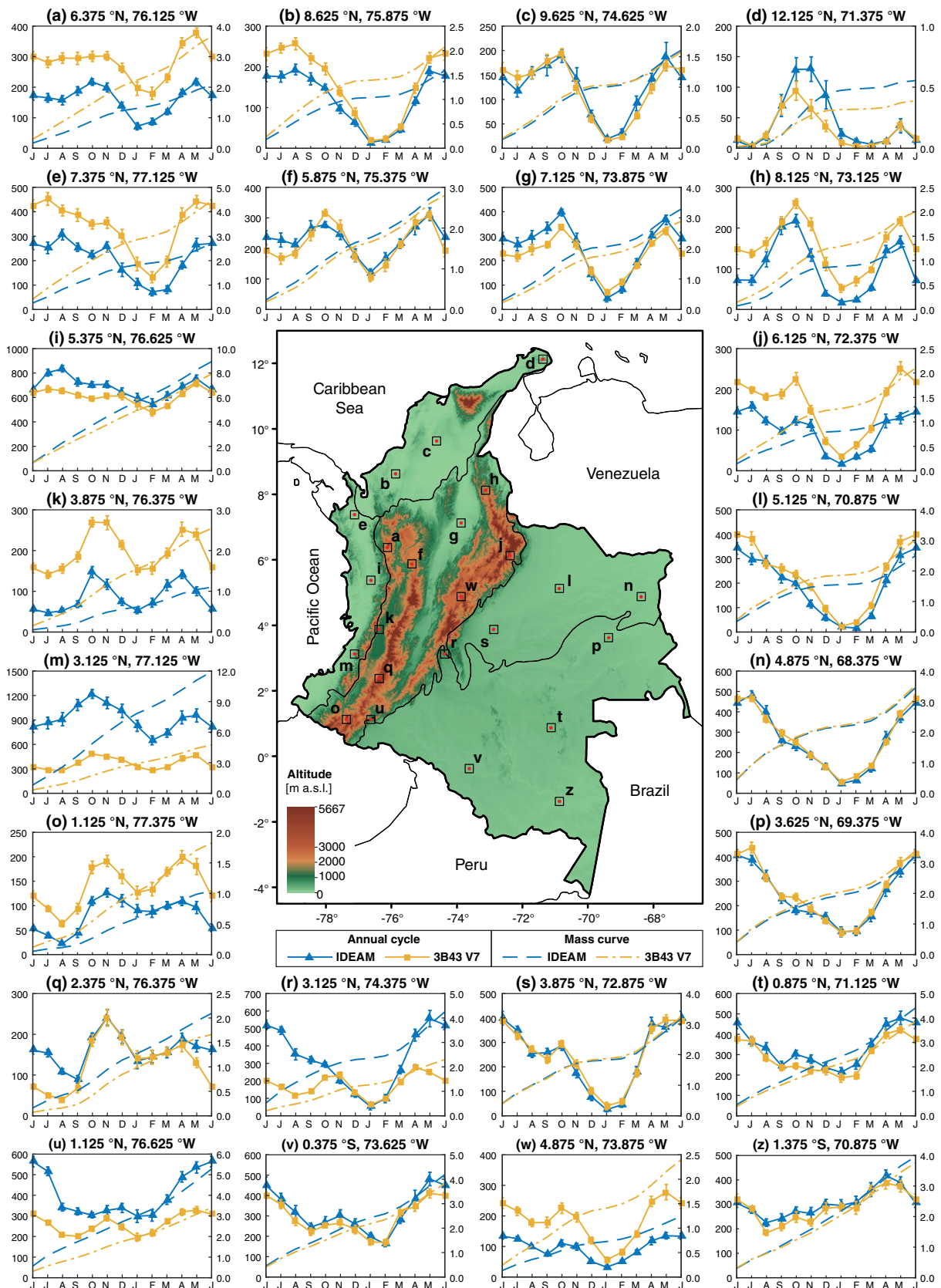


**FIGURE 3** Annual cycle and mass curve of 18-year mean precipitation at monthly resolution for 3B43 V7 and IDEAM. The mean monthly rainfall rates are shown in  $\text{mm}\cdot\text{month}^{-1}$  (left axis), and the accumulated precipitation is shown in meters (right axis) [Colour figure can be viewed at [wileyonlinelibrary.com](http://wileyonlinelibrary.com)]

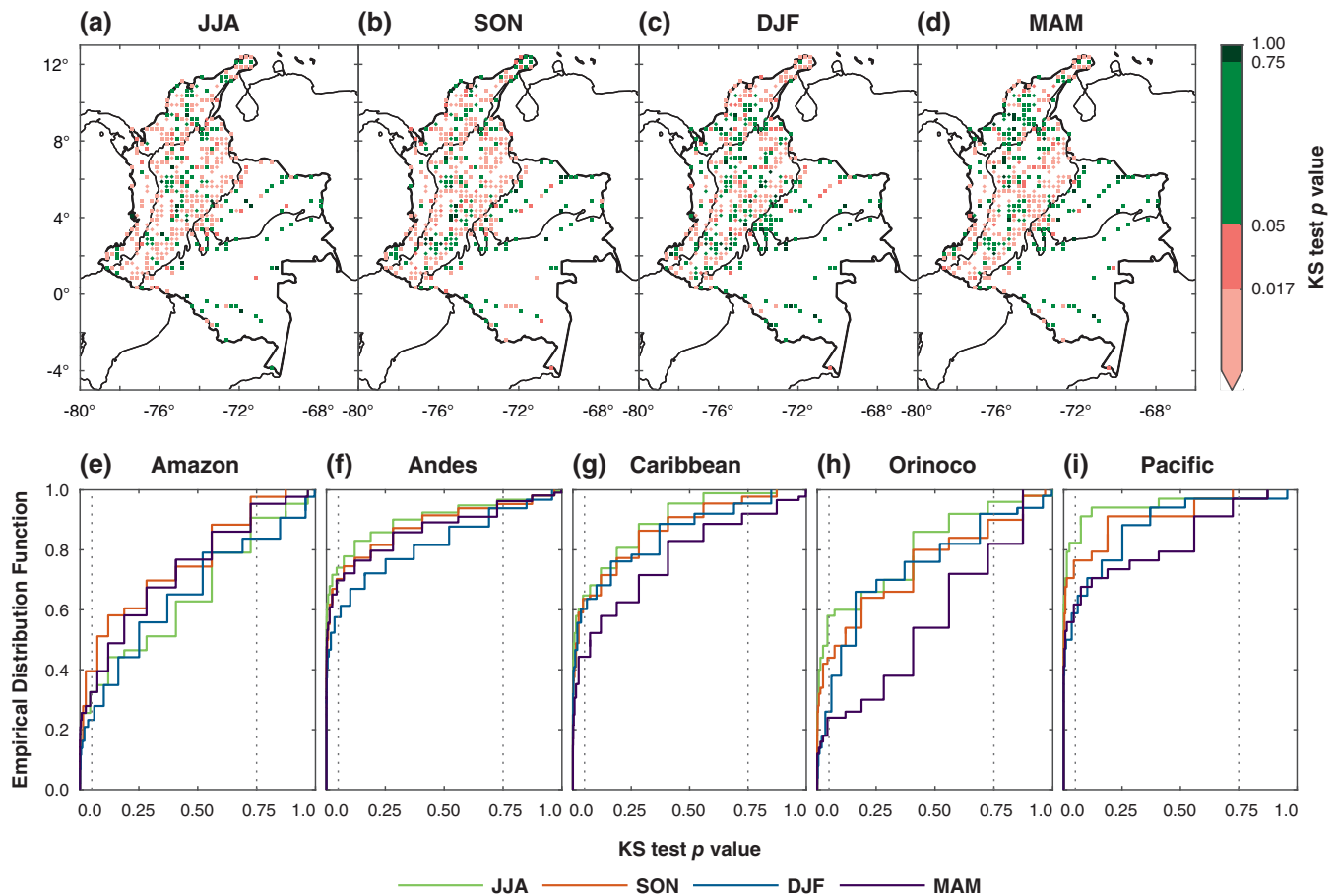


**FIGURE 4** Spatial distribution of  $\rho$ , RMSE, ME, MAE and BIAS of 3B43 V7 against IDEAM over Colombia. The pixels marked with diamonds are those with assimilated IDEAM rain gauges. All the shown values of  $\rho$  are significant at a level  $\alpha = 0.05$  [Colour figure can be viewed at [wileyonlinelibrary.com](http://wileyonlinelibrary.com)]

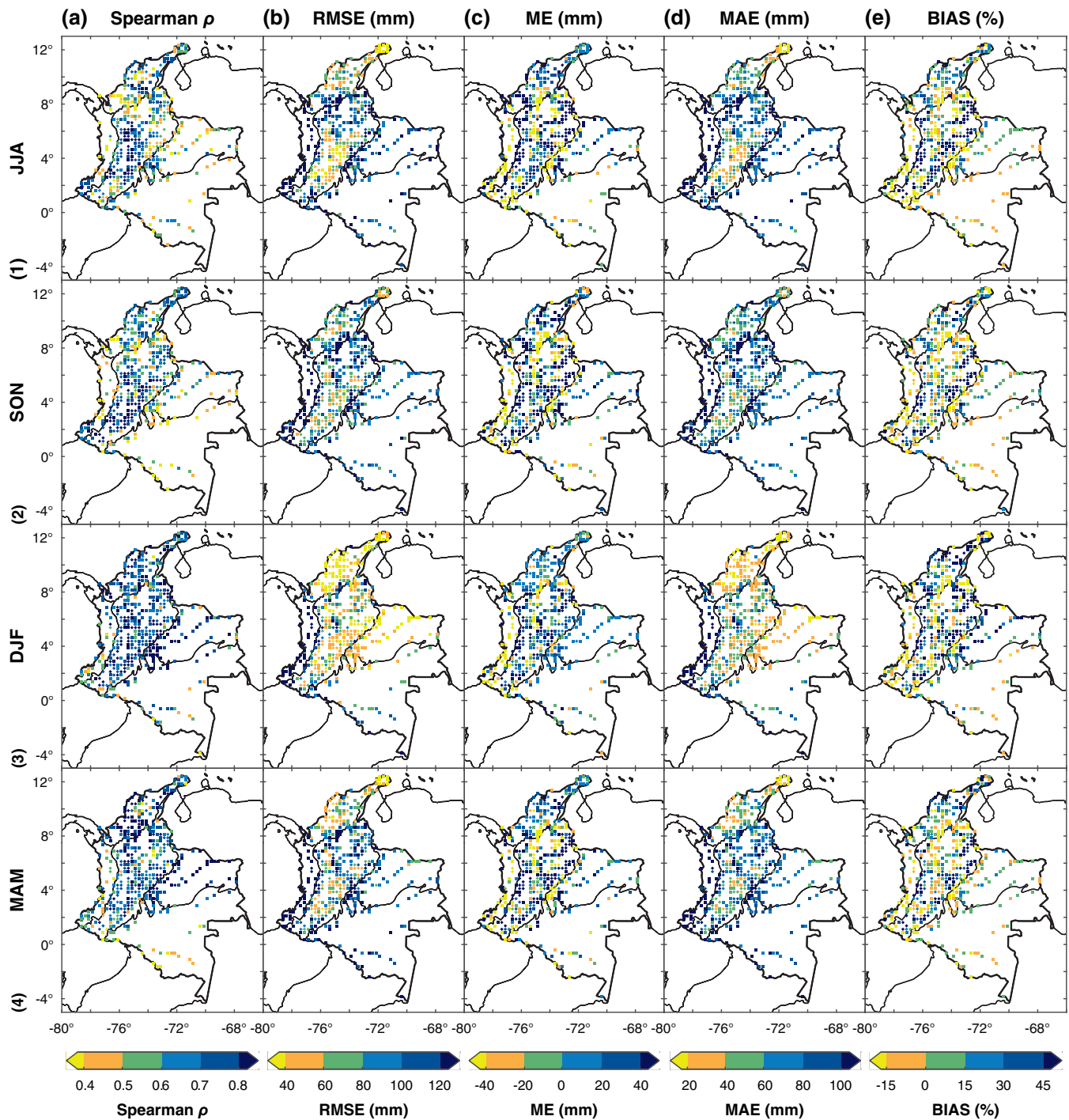
sensors. Note that although the Central Andes and the two adjacent inter-Andean valleys have an annual average rainfall of less than 1,500 mm and a bimodal annual cycle, there are overestimation errors over the inter-Andean valleys and underestimation errors over the top of the Central Range of the Andean Mountains.

Figure 5 shows scatter plots and Table 2 presents the scores of the error metrics for 3B43 V7 product during different seasons over the major natural regions of Colombia. The values of ME and BIAS lead to the conclusion that in the Amazon and Pacific (Andes and Caribbean) regions, 3B43 V7 underestimates (overestimates) the rainfall rates all year long. It can be noticed that these spatial patterns are persistent during all the seasons since the intra-annual variability of both the ME and the BIAS are due to changes in the magnitude but not in the sign of the metric. In the Orinoco region, there is underestimation during all the seasons except in DJF, when the significant overestimation may be due to the severity of the dry season there. In all regions, the magnitude of RMSE and MAE is the lowest during DJF, confirming the best overall performance of

3B43 V7 during the driest season, in terms of capturing both the average and the large rates of precipitation. Also, these two metrics have higher (lower) scores during the wet (dry) seasons in the regions with higher (lower) rainfall rates, which is a clear spatiotemporal pattern of worse performance in wet conditions. Although the Spearman rank correlation does not show such a clear temporal pattern, it exhibits an evident spatial pattern with higher (lower) values in the drier (wetter) regions. Over the Amazon and Orinoco regions,  $\rho$  also has a periodicity with higher (lower) values during dry (wet) seasons. Such a significant warm-season-based error structure has also been observed elsewhere (Chen *et al.*, 2013a, 2013b; Mantas *et al.*, 2015; Yong *et al.*, 2010).

### 4.3 | Probabilistic analysis of seasonal precipitation

The two-sample KS test is a nonparametric method to tests the null hypothesis that two empirical distribution



**FIGURE 5** Scatterplots of 3V43V7 versus IDEAM for seasonal mean monthly precipitation over the major regions of Colombia. The black line represents a 1:1 relation [Colour figure can be viewed at [wileyonlinelibrary.com](http://wileyonlinelibrary.com)]

functions are the same. It quantifies the maximum distance between the distributions and is sensitive to differences in both location and shape. The KS test result is based on the comparison of the  $p$ value, that can be interpreted as a measure of the strength of the evidence against the null hypothesis provided by the data (Wasserstein *et al.*, 2016), and the significance level  $\alpha$ , which is

the probability of rejecting the null hypothesis given that it is true, and for our purposes was taken equal to .05. If  $p \leq \alpha$ , the null hypothesis is rejected because there is evidence of statistical incompatibility with the data. Conversely, when  $p > \alpha$  and the test fails the rejection, we do not obtain any meaningful information about the veracity of the null hypothesis and therefore we cannot have

**TABLE 2** Metrics' scores obtained for the regional and seasonal validation of 3B43 V7 precipitation estimates, using all the validation pixels of each natural region of Colombia

Metric	Season	Amazon $n = 43$	Andes $n = 212$	Caribbean $n = 88$	Orinoco $n = 50$	Pacific $n = 34$
KSRR (%)	JJA	32.56	74.06	64.77	58.00	82.35
	SON	39.53	70.28	63.64	44.00	76.47
	DJF	23.26	57.55	60.23	26.00	58.82
	MAM	32.56	69.81	44.32	24.00	61.76
	JJA	0.49	0.70	0.85	0.42	0.61
	SON	0.37	0.69	0.70	0.49	0.72
Spearman ( $\rho$ )	DJF	0.77	0.73	0.74	0.83	0.63
	MAM	0.49	0.66	0.85	0.79	0.58
	JJA	131.78	108.23	87.44	137.57	290.59
RMSE ( $\text{mm}\cdot\text{month}^{-1}$ )	SON	105.48	111.34	95.96	108.34	309.12
	DJF	99.70	83.59	51.23	49.59	253.52
	MAM	143.16	107.01	71.39	117.34	259.12
	JJA	-28.44	11.24	7.08	-12.60	-103.55
	SON	-8.35	10.44	1.88	-2.56	-119.36
	DJF	-4.07	9.69	-0.38	5.41	-90.26
ME ( $\text{mm}\cdot\text{month}^{-1}$ )	MAM	-16.56	13.48	7.65	-14.30	-58.60
	JJA	95.64	77.77	60.54	101.34	212.48
	SON	79.32	81.20	71.20	82.59	213.18
	DJF	67.11	56.67	27.81	31.58	175.96
MAE ( $\text{mm}\cdot\text{month}^{-1}$ )	MAM	103.25	79.07	48.71	85.08	184.20
	JJA	-8.31	6.73	4.05	-3.60	-20.65
	SON	-3.33	4.69	0.94	-1.05	-22.13
	DJF	-2.11	7.84	-0.84	9.06	-20.41
BIAS (%)	MAM	-4.49	6.28	6.27	-5.03	-11.75

Note: All the reported values of  $\rho$  are significant at a level  $\alpha = .05$ .

statistical certainty about any conclusion (Aberson, 2002). Having all this in mind, we present the correct interpretation of the probabilistic validation of 3B43 V7.

Figure 6 shows the results of the KS test for the null hypothesis that the seasonal precipitation time series of 3B43 V7 and IDEAM are from the same empirical distribution function. Panels (a) to (d) show the spatial distribution of the seasonal  $p$  values over Colombia. Panels (e) to (i) show the empirical distribution function of the  $p$  values. The dotted lines at  $p = .05$  and  $p = .75$  are, respectively, the upper bound of the critical region (or rejection region) and the lower bound of the region with less evidence against the null hypothesis. Given that the only question that the KS test can answer is whether the data contain enough evidence to reject the null hypothesis, we have a special interest in  $p$  values very close to zero (values of  $p \leq .017$ ) that allow us to conclude, with statistical certainty, that the empirical distribution functions are different, and  $p$  values

very close to one (values of  $p > .75$ ) where the evidence against the null hypothesis is the weakest possible.

From Figure 6 and Table 2, it can be seen that in the Amazon region, during all seasons, the null hypothesis is not rejected for most pixels, with DJF (SON) being the season with the lowest (highest) KSRR, 23.26% (39.53%). In the Orinoco region, the null hypothesis is not rejected for most pixels during all the seasons but MAM, which is the wet season and the KSRR reaches a value of 58.00%. On the contrary, the null hypothesis is always rejected for most pixels of the Pacific and Andes regions, in greater (lower) proportion during JJA (DJF) with KSRR of 82.35 and 74.06% (58.82% and 57.55%), respectively. Finally, in the Caribbean region, the null hypothesis is rejected for most pixels during all the seasons but MAM, when the KSRR decreases to a value of 44.32%. These results exhibit the same spatial and temporal patterns of the other metrics, with better (worse) scores during the

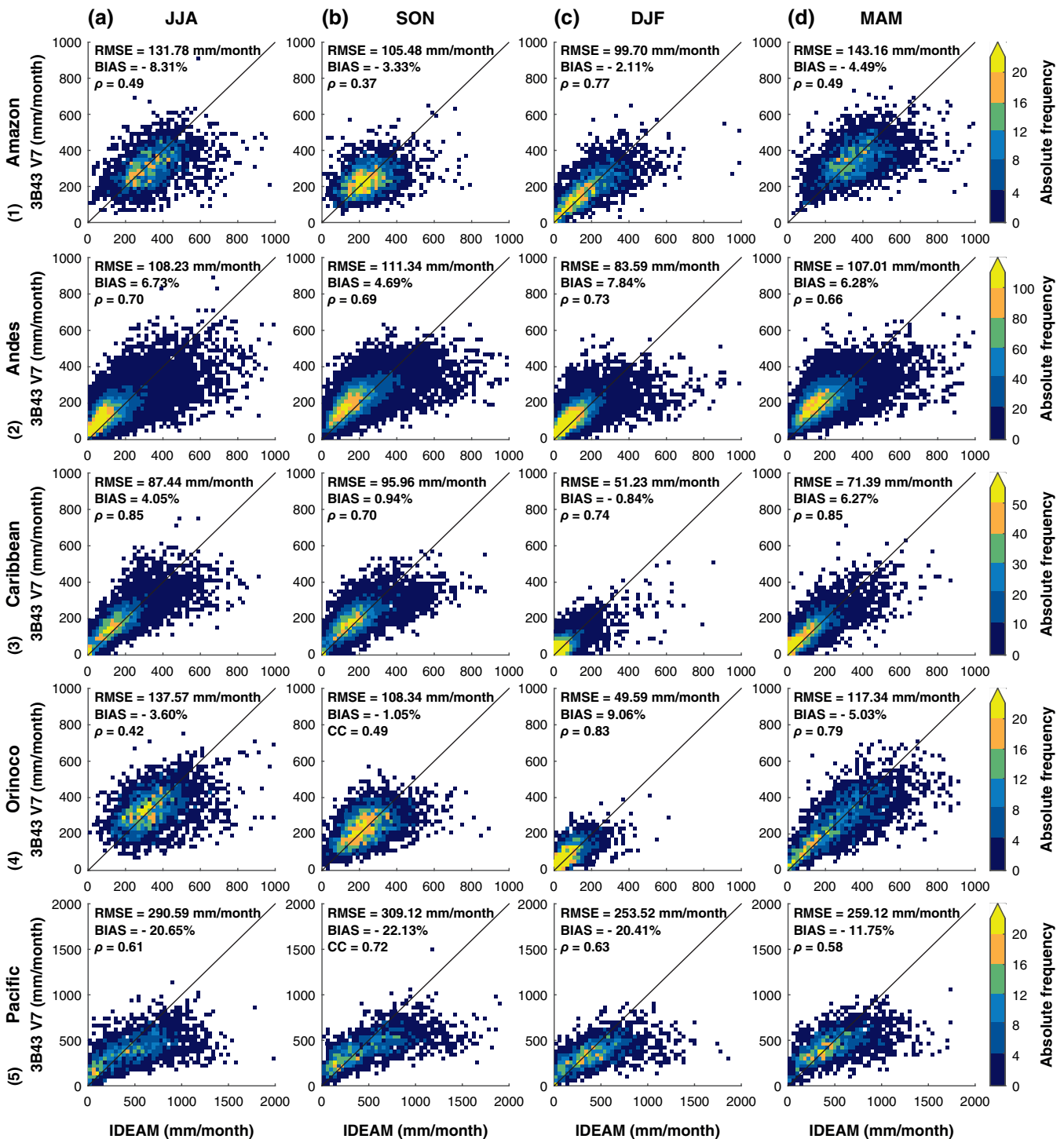


**FIGURE 6** Seasonal evaluation of the  $p$  value of the KS test for the null hypothesis that the precipitation time series at monthly resolution of IDEAM and 3B43 V7 are from the same empirical distribution function. (a–d) Spatial distribution of  $p$  values and (e–i) regional empirical distribution functions over the five major natural regions of Colombia. The pixels marked with diamonds in panels (a–d) are those with assimilated IDEAM rain gauges. Dotted vertical lines at  $p = .05$  and  $p = .75$  are, respectively, the upper bound of the rejection region and the lower bound of the region with less evidence against the null hypothesis [Colour figure can be viewed at [wileyonlinelibrary.com](http://wileyonlinelibrary.com)]

dry (wet) season, better performance over the low-lying and mostly plain regions and significant difficulties over regions with complex topography or intense rainfall regimes. Regarding the statistical significance, although

there are regions and seasons with a non-rejection rate greater than that of rejection, in all cases the  $p$  values greater than .75 occur in less than 20% of the validation sites. Those  $p$  values correspond to



the pixels with the highest compatibility between the data and the null hypothesis and constitute the minority of non-rejection cases. It is remarkable that in the Pacific region, dark green pixels are almost nonexistent during all seasons. This implies that

there is a high statistical uncertainty for the case of null results over the entire country. Conversely, most of the pixels where the null hypothesis is rejected are light pink and have  $p$  values less than or equal to .017, which means that the rejection of the null

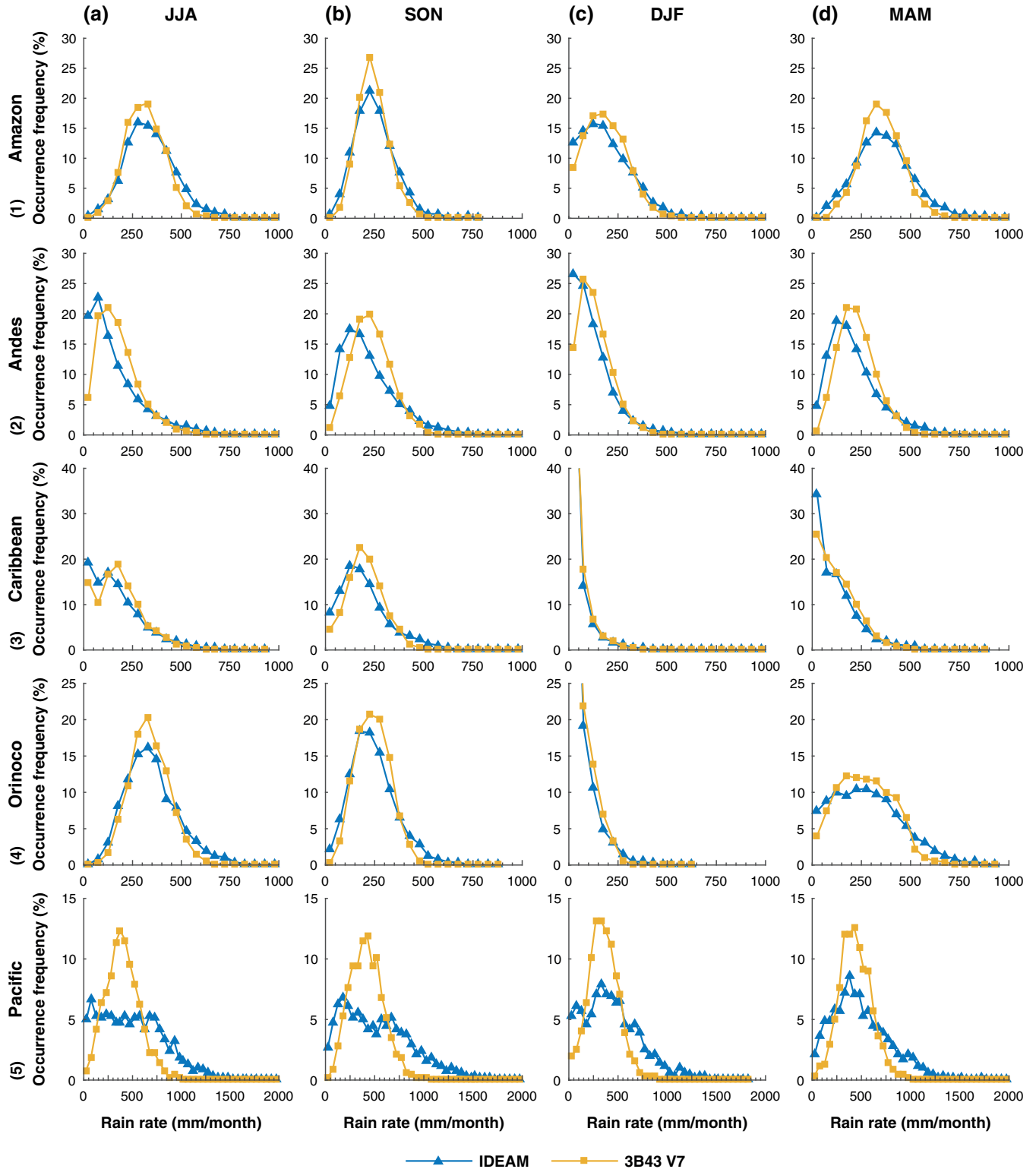


**FIGURE 7** Seasonal and regional evaluation of precipitation occurrence frequency of IDEAM and 3B43 V7 as a function of the mean monthly rainfall rate with a  $50 \text{ mm-month}^{-1}$  interval [Colour figure can be viewed at [wileyonlinelibrary.com](http://wileyonlinelibrary.com)]

hypothesis is concluded with strong statistical certainty and that 3B43 V7 has difficulties capturing both the location and the shape of the distribution function of rainfall rates.

#### 4.4 | Probability distributions by occurrence

PDFs can be used to validate the rainfall amount distribution and the error dependence on the precipitation rate for satellite estimates (Tian *et al.*, 2010; Chen *et al.*, 2013b). Figure 7 shows the PDF by occurrence as a function of monthly precipitation for each season and over the major regions of Colombia. At this temporal timescale, rainfall records are always greater than zero for both 3B43 V7 and IDEAM, therefore all the validation pixels were used to compute the PDF. As shown in Figure 7, the 3B43 V7 is able to capture the location and shape of the distribution in the Amazon, Caribbean and Orinoco regions, with better performance during DJF. Over the Andes region, the satellite product captures the shape but always overestimates the location, while in the Pacific region the performance of 3B43 V7 is very poor all year long, especially because the distribution of gauged rainfall rates has a heavy tail that is not captured by the satellite product. In all the studied regions the frequency of rainfall is overestimated, between rates from 350 to 550 mm·month<sup>-1</sup> for the Pacific and 200 to 400 mm·month<sup>-1</sup> for the other regions. In the Amazon and Orinoco, there is also frequency underestimation for rainfall rates more than 500 mm·month<sup>-1</sup> during the wet seasons. In the Pacific, this underestimation of heavy rainfall frequency is more significant all year long and occurs for exceptionally large rates between 650 and 1,200 mm·month<sup>-1</sup>. Underestimation of frequency for light rainfall with rates less than 50 mm·month<sup>-1</sup> is significant over the Andes and Pacific regions and increases during the dry seasons. These results show that the overall underestimation (overestimation) observed in the Andes (Pacific) region can be primarily attributed to the inability to detect very frequent light rainfall events and less frequent but very heavy storms.

## 5 | DISCUSSION

### 5.1 | Uncertainty sources

We have performed a regional validation of 3B43 V7 product over Colombia, a country with very complex topography given the branching of the Andes mountain range and very diverse precipitation regimes due to the

multiple climatic drivers involved in the rainfall production. The Pacific region is the rainiest place of Colombia and arguably of the world (Poveda and Mesa, 2000), with pixels reporting monthly mean precipitation rates of more than 800 mm·month<sup>-1</sup>. It is followed by the Amazon and Orinoco regions albeit with significantly lower rainfall amounts. The Caribbean and Andes regions are the driest (Álvarez-Villa *et al.*, 2011). The seasonal variability of precipitation in Colombia is mainly modulated by the meridional migration of the ITCZ. The Andes, Caribbean and Pacific regions have a bimodal annual cycle, with wet (dry) seasons in MAM and SON (JJA and DJF), while the Orinoco and Amazon regions exhibit unimodal annual cycles with a single dry season during DJF. Despite the differences, it is worth noting that DJF is the driest season for all regions of the country, which can be explained by the southern migration of the ITCZ and the weakening of the Choco Jet.

Concerning the phase of the annual cycle of mean precipitation, the performance of 3B43 V7 product is outstanding, which has been credited to the incorporation of gauge information during processing at monthly timescale (Su *et al.*, 2008; Scheel *et al.*, 2011; Mantas *et al.*, 2015). Regarding the amplitude of the annual cycle, over the entire country the scores of the error metrics are better (worse) during the dry (wet) season. In general, 3B43 V7 captured the spatial patterns of regional variability, however, there is an evident underestimation (overestimation) in precipitation amounts over the Pacific (Andes) region. This dependence of TMPA products performance on rainfall intensity has been widely observed for every timescale. In particular, over regions of South America with similar climatic features, it is well known that satellite products underestimate (overestimate) precipitation in areas of high (low) rainfall rates during wet (dry) seasons (Dinku *et al.*, 2010b; Condom *et al.*, 2011; Mantas *et al.*, 2015; Erazo *et al.*, 2018; Palomino-Ángel *et al.*, 2019).

Specifically, there are overestimation errors in the driest places of the country, with annual average rainfall between 300 and 1,500 mm, such as the tops of the Western and the Eastern Andes and most of the Caribbean region. TMPA products overestimation over the dry areas of South America has been attributed to subcloud evaporation (Dinku *et al.*, 2010b; Erazo *et al.*, 2018). In Colombia during DJF, the overestimation gets more severe in the Caribbean and Orinoco regions. This result along with the dramatic decrease in rainfall rates during this season supports the hypothesis of the subcloud evaporation as the cause of the overestimation (Dinku *et al.*, 2010b, 2011; Erazo *et al.*, 2018).

Conversely, underestimation errors are found in the rainiest areas of the country, those that have rainfall

regimes of more than 3,000 mm per year (Poveda *et al.*, 2007; Álvarez-Villa *et al.*, 2011) and are covered by tropical rainforests or located on wetlands, such as the southeastern part of the Amazon region, the eastern piedmont of the Eastern Andes, the Pacific region and the Mompox depression region located between the central Caribbean and the Northern Andes regions. Most of the rainfall in these areas is driven by orography and convection, which tends to be deeper where land-atmosphere interactions occur. For example, the warm rainfall in the Eastern and the Western piedmonts of the Andes is the result of the orographic uplift of the CLLJ and CAO, and the Choco low-level jets, which bring the moisture from the Amazon Basin and the Pacific Ocean, respectively (Poveda *et al.*, 2014; Bedoya-Soto *et al.*, 2019). Over these slopes, 3B43 V7 exhibits a significant underestimation (Figure 3m,r,u) that can be attributed to the well-documented limitations of the PR to capture the rainfall rates of intense convective warm precipitation (Iguchi *et al.*, 2000; Dinku *et al.*, 2010b; Condom *et al.*, 2011; Rasmussen *et al.*, 2013; Mantas *et al.*, 2015; Erazo *et al.*, 2018). However, it is remarkable that the underestimation is much more significant in the Western piedmont than in the Eastern piedmont. This is because the convective clouds are higher in the Pacific region and the VIRS, which provides information of cloud-top height, has a better performance correlating the low-level short convection with the ground precipitation (Erazo *et al.*, 2018). These difficulties of the sensors with the deep convection may be the main reason for the exceptionally high scores of the error metrics in the Pacific region.

On the other hand, mountainous regions are especially challenging for remote precipitation measurements. Even though the Central Andes and the two adjacent inter-Andean valleys have an annual average rainfall of less than 1,500 mm and a bimodal annual cycle, there are overestimation errors over the inter-Andean valleys and underestimation errors over the top of the Central Range of the Andean Mountains. This behavior can be understood considering that the TMPA algorithm estimates rainfall through an inverse approach from the brightness temperature at the cloud top (Levizzani *et al.*, 2002). The presence of complex topography affects the processing scheme of microwave and IR data seen from space, which are strongly dependent on the surface type (Mätzler and Standley, 2000; Scheel *et al.*, 2011; Mantas *et al.*, 2015). The highly heterogeneous terrain with varying brightness temperatures over the Andes causes a strong scattering of the electromagnetic waves emitted by the PR, which constitutes a large source of error for rainfall estimations (Mourre *et al.*, 2015; Satgé *et al.*, 2016). Moreover, rain retrieval algorithms misidentify cold surfaces and ice cover over the

mountain-tops of the Colombian Andes as raining clouds, contributing to the overestimation errors (Dinku *et al.*, 2010a).

However, the accuracy of satellite estimates also depends on the skill of the sensors to capture the frequency of different precipitation intensities (Tian *et al.*, 2010; Chen *et al.*, 2013b). Our results show that the overall underestimation (overestimation) observed over the Andes (Pacific) region can be primarily attributed to the inability to detect very frequent light rainfall events and less frequent but very heavy storms. Underestimation of large precipitation rates frequencies has also been observed in the Peruvian Andes, the Continental United States and mountainous regions of China (Yong *et al.*, 2010; Chen *et al.*, 2013a; Mantas *et al.*, 2015). Underestimation of light rainfall frequencies has also been reported in semiarid basins and mountainous regions of China (Yong *et al.*, 2010; Chen *et al.*, 2013a). These difficulties to detect the occurrence of precipitation events have been attributed to the discrete sampling and the small swath width of PR that cause the light and heavy rainfall of short duration to be missed from space (Condom *et al.*, 2011).

Finally, the magnitude of the errors is also related to the discrete temporal sampling of satellite instruments and the scale differences between precipitation data sets used for validation. Many theoretical studies have shown that there are errors ranging from  $\pm 8\%$  to  $\pm 12\%$  in the monthly estimations due to the discrete temporal sampling (Shin and North, 1988; North and Nakamoto, 1989; Bell *et al.*, 1990). Also, Yong *et al.* (2010) reported that when gridded products are directly compared with point-scale gauged data, the spatial-scale differences contribute to the evaluation errors.

## 5.2 | Related approaches in the literature

A large number of studies have been carried out to validate TMPA products, especially in places with complex topography or in regions under the influence of the same macro climatic features of Colombia. See Table 3 for a review of the most relevant ones, which have validated precipitation estimates using the same error metrics considered in this paper, at the same temporal resolution. If a seasonal or regional validation was performed, the worst score of the metric is reported for comparative purposes. All these previous studies have concluded that the temporal variability of mean rainfall is properly captured by the TRMM satellite products. This is, the phase of the annual cycle coincides since the wet and dry months are the same, both in the rain gauges and the satellite

**TABLE 3** Review of the most relevant studies, which have validated precipitation estimates of TRMM using the same error metrics that we considered, at the same temporal resolution. If a seasonal or regional validation was performed, the worst score of the metric is reported for comparative purposes

Reference	Study region	TRMM product	Validation period	Ground truth		Metrics					
				Number of rain gauges	Data source	Pearson $r$	RMSE	ME	MAE	BIAS (%)	
Ballari <i>et al.</i> (2016)	Ecuador	3B43 V7	1998–2010	14	INAMHI	$\geq 0.75$	$\leq 88.49$	$\leq 27.89$			
Chen and Li (2016)	China	3B43 V7	March 2014–February 2015	>750	CMA	$\geq 0.86$	$\leq 61.71$				$\leq 24.18$
Danelichen <i>et al.</i> (2013)	Midwest region in Brazil	3B43 V6	2000–2010	5	ICEA	$\rho \geq 0.82^a$	$\leq 71.02$			$\leq 46.43$	
Dinku <i>et al.</i> (2007)	Ethiopia	3B43 <sup>b</sup>	1998–2004	120 <sup>c</sup>	NMA	0.92		-12.00			-8.00
Duan <i>et al.</i> (2016)	Adige basin in Italy	3B42 V7 <sup>d</sup>	2000–2010	101 <sup>c</sup>	APT and APB	0.84	32.16	9.74	23.93		13.00
Duan <i>et al.</i> (2012)	Caspian Sea region in Iran	3B43 V6	1999–2003	39	IRIMO	0.73	37.84				7.00
Erazo <i>et al.</i> (2018)	Pacific slope and coast of Ecuador	3B43 V7	1998–2010	325 <sup>c</sup>	INAMHI	0.82					-2.80
Franchito <i>et al.</i> (2009)	Brazil	3A25 V5	1998–2000	Dense network	ANEEL	$\geq 0.37$	$\leq 152.50$	$\geq -66.70 \leq 97.40$			$\geq -47.80 \leq 75.40$
Hu <i>et al.</i> (2014)	Ganjiang basin in China	3B43 V6	2003–2009	325 <sup>c</sup>	JPHB	0.94		8.90	25.40		7.50
Karaseva <i>et al.</i> (2012)	Kyrgyzstan	3B43 V6	1998–2007	35	KHMA	$\geq 0.54$	$\leq 82.21$	$\geq -21.66 \leq 18.70$			
Mantas <i>et al.</i> (2015)	Andes mountain range in Peru	3B42 V7 <sup>d</sup>	2000–2012	38	SENAMHI	$\geq 0.70$	$\leq 64.65$				$\leq 73.00$
Scheel <i>et al.</i> (2011)	Cusco region in Peru	3B42 V6 <sup>d</sup>	Jan 1998–May 2008	4	SENAMHI	0.91	24.14				
Yong <i>et al.</i> (2010)	Laohahe basin in China	3B42 V6 <sup>d</sup>	2000–2005	53		0.93	18.72	6.53	11.63		19.19

Abbreviations: ANEEL, Agência Nacional de Energia Elétrica; APT and APB, Autonomous Province of Trento and Autonomous Province of Bolzano, respectively; CMA, China Meteorological Administration; ICEA, Instituto de Controle de Espaço Aéreo; INAMHI, Instituto Nacional de Meteorología e Hidrología de Ecuador; IRIMO, Islamic Republic of Iran Meteorological Organization; JPHB, Jiangxi Province Hydrology Bureau; KHMA, Kyrgyz Hydro-Meteorology Agency; NMA, National Meteorological Agency of Ethiopia; SENAMHI, Servicio Nacional de Meteorología e Hidrología del Perú.

<sup>a</sup>Spearman rank correlation.

<sup>b</sup>TRMM product version not specified.

<sup>c</sup>Interpolated into a gridded database.

<sup>d</sup>Aggregated to monthly timescale.

**TABLE 4** Metrics' scores obtained for the seasonal and regional validation of 3B43 V7 precipitation estimates, using only the pixels with assimilated IDEAM rain gauges of the Andes and Caribbean regions

Metric	Season	Andes $n = 106$	Caribbean $n = 19$
KSRR (%)	JJA	80.19	68.42
	SON	74.53	63.16
	DJF	60.38	36.84
	MAM	74.53	36.84
Spearman ( $\rho$ )	JJA	0.71	0.74
	SON	0.72	0.63
	DJF	0.75	0.80
	MAM	0.68	0.84
RMSE ( $\text{mm}\cdot\text{month}^{-1}$ )	JJA	95.62	71.64
	SON	92.24	75.47
	DJF	71.41	34.48
	MAM	92.92	53.17
ME ( $\text{mm}\cdot\text{month}^{-1}$ )	JJA	21.98	16.71
	SON	25.25	5.91
	DJF	18.34	2.95
	MAM	24.44	10.32
MAE ( $\text{mm}\cdot\text{month}^{-1}$ )	JJA	71.24	54.28
	SON	70.13	58.68
	DJF	50.22	21.59
	MAM	71.39	39.15
BIAS (%)	JJA	15.64	9.45
	SON	13.11	2.98
	DJF	15.90	7.09
	MAM	12.49	8.34

Note: All the reported values of  $\rho$  are significant at a level  $\alpha = .05$ .

databases. However, the rainfall amounts are underestimated (overestimated) during dry (wet) seasons. Also, the dependence of the performance on precipitation intensity was observed everywhere, with overestimation (underestimation) of heavy (light) rainfall events. Like all the previous studies in South America, our results report underestimation errors along the South American Pacific coast, whereas overestimation over the Andes and better performance on the Amazon rainforest. When compared to studies in mountainous regions, there is a persistent result of better performance at low elevations. However, in terms of the metrics' scores, in Colombia the 3B43 V7 product reaches the lowest  $\rho$  and the highest RMSE, and arguably the worst performance of the entire globe. In the Colombian Pacific coast, the RMSE is greater than  $253.52 \text{ mm}\cdot\text{month}^{-1}$  and  $\rho$  is less than 0.72. In the Colombian Andes, the RMSE is higher than  $83.59 \text{ mm}\cdot\text{month}^{-1}$  and  $\rho$  is lower than 0.73. These bad scores can be attributed to the special physical and

climatic characteristics of the country, namely, the greater complexity of the topography over the Colombian Andes caused by the branching of the mountain range and the aforementioned exceptionally high rainfall regime of the Colombian Pacific region.

### 5.3 | Non-independent pixels validation

Table 4 reports the scores of the error metrics (Table 1) for 3B43 V7 pixels with assimilated IDEAM rain gauges, over the Andes and Caribbean regions, where most of such pixels are located. The improvement in  $\rho$ , RMSE and MAE score is evident. However, the increase of ME and BIAS score implies a greater overestimation over the non-independent pixels. These results indicate that in the non-assimilated rain gauges of the Andes and Caribbean regions, the bias correction with GPCC gauge analysis decreases the standard deviation of the errors due to a



magnitude reduction of the large biases in the precipitation estimates, albeit no improvement is observed in the estimation of the mean rainfall rate, which was expected given the high spatial variability of the precipitation. In terms of the rejection rate of the KS test, over the non-independent pixels of the Amazon and Caribbean regions, the bias correction with GPCC gauge analysis improves the estimation of the shape but increases the bias in the location of the distribution function of rainfall rates, which results in worse scores for the KSRR metric.

## 6 | CONCLUSIONS

In this study, we have validated precipitation estimates of the 3B43 V7 satellite product with respect to in situ measurements of monthly rainfall at 1180 rain gauges over Colombia, at monthly and seasonal timescales, during the 1998–2015 period. The principal findings are summarized as follows:

- 1 The 3B43 V7 satellite product is able to capture the phase of the annual cycle of mean precipitation at monthly resolution, both for unimodal or bimodal regimes over the five major regions of Colombia. However, regarding the amplitude, we identified significant discrepancies, with persistent spatial and temporal patterns that seem to be strongly related to the topography and climatology of each region of the country. In general, underestimation (overestimation) errors have been found in the rainiest (driest) areas of the country, with considerable magnitudes over the Andes (Pacific) region. The discrepancies between satellite estimates and gauged data are larger at the highest elevations over the Andes region and tend to decrease reaching a notable agreement over the low-lying and mostly plain Orinoco and Amazon regions.
- 2 The temporal discrete sampling technique and the small swath width of some instruments on board TRMM satellite have caused difficulties to detect the occurrence of short-duration precipitation events. In particular, we have found that 3B43 V7 product misses very frequent light rainfall events and less frequent but very heavy storms, which contribute to the overall underestimation (overestimation) observed over the Andes (Pacific) region.
- 3 Due to the assimilation of gauge information at monthly timescale during the processing of 3B43 V7, temporal patterns in the metrics' scores exhibit the same seasonality of the annual cycle of mean precipitation of each region. In general, the performance of the satellite product over Colombia gets worsened (improved) during the wet (dry) seasons.
- 4 These spatial and temporal patterns have been reported over regions all around the globe, where the climatic or topographic features are similar to Colombia. However, in terms of the metrics' scores, over Colombia 3B43 V7 exhibits the worst performance. This can be attributed mainly to the greater complexity of the Colombian Andes caused by the three branches of the mountain range and the exceptionally high rainfall regime in the Colombian Pacific region. This particular coexistence of very especial topographic and climatic features amplifies the well-documented limitations of VIRS and PR when sensing intense convective warm precipitation caused by complex land-atmosphere interactions over highly heterogeneous terrain.
- 5 The error characteristics identified and quantified in this study will have significant implications for hydrological applications and techniques of remote rainfall sensing. Our results suggest that the gauge-based bias-correction of the research quality version products of TMPA V7 is not sufficient to assess the well-documented limitations of the sensors used to estimate precipitation from space. Not even when a dense network of gauged data is assimilated to produce monthly scale estimates, as in the case of 3B43 V7 product over Colombia. Our findings constitute a warning about the major challenges faced when complex climatic and physiographic features are present in the same area and can contribute to improving the algorithms of future rainfall missions

## ACKNOWLEDGEMENTS

We are grateful to the HERMES program of Universidad Nacional de Colombia at Medellín, for funding this work through the grant no. 35973. We thank IDEAM and NASA for providing the gauge and satellite datasets used in this study. We are also grateful to two anonymous reviewers for their constructive comments on our manuscript. This study is a result of the project 'Validation of the TRMM and GPM Precipitation Products Using Information from Rain Gauges in Colombia', developed in cooperation between Universidad Nacional de Colombia at Medellín, IDEAM and NASA, and makes part of the Precipitation Measurement Missions (PMM) Research Program.

## ORCID

Sara M. Vallejo-Bernal  <https://orcid.org/0000-0003-3134-0449>

Viviana Urrea  <https://orcid.org/0000-0002-2971-2656>

Juan M. Bedoya-Soto  <https://orcid.org/0000-0003-3066->

9306

Daniela Posada  <https://orcid.org/0000-0002-3711-0516>Walter A. Petersen  <https://orcid.org/0000-0002-6090-7144>George J. Huffman  <https://orcid.org/0000-0003-3858-8308>Germán Poveda  <https://orcid.org/0000-0002-7907-6360>

## REFERENCES

- Aberson, C. (2002) Interpreting null results: improving presentation and conclusions with confidence intervals. *Journal of Articles in Support of the Null Hypothesis*, 1(3), 36–42.
- Adeyewa, Z.D. and Nakamura, K. (2003) Validation of TRMM radar rainfall data over major climatic regions in Africa. *Journal of Applied Meteorology*, 42(2), 331–347.
- Álvarez-Villa, O.D., Vélez, J.I. and Poveda, G. (2011) Improved long-term mean annual rainfall fields for Colombia. *International Journal of Climatology*, 31(14), 2194–2212.
- Amador, J.A. (1998) A climatic feature of the tropical Americas: the trade wind easterly jet. *Tópicos Meteorológicos y Oceanográficos*, 5(2), 91–102.
- Amador, J.A. (2008) The intra-Americas sea low-level jet: overview and future research. *Annals of the New York Academy of Sciences*, 1146(1), 153–188.
- Amador, J.A. and Magaña, V. (1999) Dynamics of the low-level jet over the Caribbean Sea. In: *Preprints 23rd Conference on Hurricanes and Tropical Meteorology*. Dallas, USA: American Meteorological Society, 868–869.
- Arkin, P.A. and Ardanuy, P.E. (1989) Estimating climatic-scale precipitation from space: a review. *Journal of Climate*, 2(11), 1229–1238.
- Ballari, D., Castro, E. and Campozano, L. (2016) Validation of satellite precipitation TRMM 3B43 in Ecuadorian coastal plains, Andean highlands and Amazonian rainforest. *International Archives of the Photogrammetry, Remote Sensing & Spatial Information Sciences*, XLI-B8, 305–311.
- Becker, A., Finger, P., Meyer-Christoffer, A., Rudolf, B., Schamm, K., Schneider, U. and Ziese, M. (2013) A description of the global land-surface precipitation data products of the Global Precipitation Climatology Centre with sample applications including centennial (trend) analysis from 1901–present. *Earth System Science Data*, 5(1), 71–99.
- Bedoya-Soto, J., Aristizabal, E., Carmona, A.M. and Poveda, G. (2019) Seasonal shift of the diurnal cycle of rainfall over Medellín's valley, Central Andes of Colombia (1998–2005). *Frontiers in Earth Science*, 7, 92.
- Bell, T.L., Abdullah, A., Martin, R.L. and North, G.R. (1990) Sampling errors for satellite-derived tropical rainfall: Monte Carlo study using a space-time stochastic model. *Journal of Geophysical Research: Atmospheres*, 95(D3), 2195–2205.
- Berbery, E.H. and Collini, E.A. (2000) Springtime precipitation and water vapor flux over southeastern South America. *Monthly Weather Review*, 128(5), 1328–1346.
- Biasutti, M., Yuter, S.E., Burleyson, C.D. and Sobel, A.H. (2012) Very high resolution rainfall patterns measured by TRMM precipitation radar: seasonal and diurnal cycles. *Climate Dynamics*, 39(1–2), 239–258.
- Bolvin, D. and Huffman, G. (2015) Transition of 3B42/3B43 research product from monthly to climatological calibration/adjustment. *NASA Precipitation Measurement Missions Document*. Washington, DC, USA: NASA, pp. 1–11.
- Candès, E.J. and Recht, B. (2009) Exact matrix completion via convex optimization. *Foundations of Computational Mathematics*, 9(6), 717–772.
- Chen, F. and Li, X. (2016) Evaluation of IMERG and TRMM 3B43 monthly precipitation products over mainland China. *Remote Sensing*, 8(6), 472.
- Chen, S., Hong, Y., Cao, Q., Gourley, J.J., Kirstetter, P.-E., Yong, B., Tian, Y., Zhang, Z., Shen, Y., Hu, J. and Hardy, J. (2013a) Similarity and difference of the two successive V6 and V7 TRMM multisatellite precipitation analysis performance over China. *Journal of Geophysical Research: Atmospheres*, 118(23), 13,060–13,074.
- Chen, S., Hong, Y., Gourley, J.J., Huffman, G.J., Tian, Y., Cao, Q., Yong, B., Kirstetter, P.-E., Hu, J., Hardy, J., Li, Z., Khan, S.I. and Xue, X. (2013b) Evaluation of the successive V6 and V7 TRMM multisatellite precipitation analysis over the Continental United States. *Water Resources Research*, 49(12), 8174–8186.
- Christian, H. J., Blakeslee, R. J., and Goodman, S. J. (1992) Lightning Imaging Sensor (LIS) for the Earth Observing System. *NASA Technical Memorandum 4350*. Huntsville, USA: Marshall Space Flight Center.
- Collischonn, B., Collischonn, W. and Tucci, C.E.M. (2008) Daily hydrological modeling in the Amazon basin using TRMM rainfall estimates. *Journal of Hydrology*, 360(1–4), 207–216.
- Condom, T., Rau, P. and Espinoza, J.C. (2011) Correction of TRMM 3B43 monthly precipitation data over the mountainous areas of Peru during the period 1998–2007. *Hydrological Processes*, 25(12), 1924–1933.
- Curtis, S., Salahuddin, A., Adler, R.F., Huffman, G.J., Gu, G. and Hong, Y. (2007) Precipitation extremes estimated by GPCP and TRMM: ENSO relationships. *Journal of Hydrometeorology*, 8(4), 678–689.
- Danelichen, V.H.d.M., Machado, N.G., Souza, M.C. and Biudes, M. S. (2013) TRMM satellite performance in estimated rainfall over the Midwest region of Brazil. *Revista Brasileira de Climatologia*, 12(1), 22–31.
- Derin, Y., Anagnostou, E., Berne, A., Borga, M., Boudevillain, B., Buytaert, W., Chang, C.-H., Delrieu, G., Hong, Y., Hsu, Y.C., Lavado-Casimiro, W., Manz, B., Moges, S., Nikolopoulos, E.I., Sathu, D., Salerno, F., Rodríguez-Sánchez, J.P., Vergara, H.J. and Yilmaz, K.K. (2016) Multiregional satellite precipitation products evaluation over complex terrain. *Journal of Hydrometeorology*, 17(6), 1817–1836.
- Derin, Y. and Yilmaz, K.K. (2014) Evaluation of multiple satellite-based precipitation products over complex topography. *Journal of Hydrometeorology*, 15(4), 1498–1516.
- Dinku, T., Ceccato, P. and Connor, S.J. (2011) Challenges of satellite rainfall estimation over mountainous and arid parts of East Africa. *International Journal of Remote Sensing*, 32(21), 5965–5979.
- Dinku, T., Ceccato, P., Grover-Kopec, E., Lemma, M., Connor, S. and Ropelewski, C. (2007) Validation of satellite rainfall products over East Africa's complex topography. *International Journal of Remote Sensing*, 28(7), 1503–1526.
- Dinku, T., Connor, S.J. and Ceccato, P. (2010a) Comparison of CMORPH and TRMM-3B42 over mountainous regions of

- Africa and South America. In: Gebremichael, M. & Hossain, F. (Eds.) *Satellite Rainfall Applications for Surface Hydrology*. Dordrecht, Netherlands: Springer, pp. 193–204.
- Dinku, T., Ruiz, F., Connor, S.J. and Ceccato, P. (2010b) Validation and intercomparison of satellite rainfall estimates over Colombia. *Journal of Applied Meteorology and Climatology*, 49(5), 1004–1014.
- Duan, Z., Bastiaanssen, W. and Liu, J. (2012) Monthly and annual validation of TRMM Multisatellite Precipitation Analysis (TMPA) products in the Caspian Sea region for the period 1999–2003. In: *Proceedings of International Geoscience and Remote Sensing Symposium (IGARSS)*. Munich, Germany: IEEE, pp. 3696–3699.
- Duan, Z., Liu, J., Tuo, Y., Chiogna, G. and Disse, M. (2016) Evaluation of eight high spatial resolution gridded precipitation products in Adige Basin (Italy) at multiple temporal and spatial scales. *Science of the Total Environment*, 573, 1536–1553.
- Ebert, E.E., Janowiak, J.E. and Kidd, C. (2007) Comparison of near-real-time precipitation estimates from satellite observations and numerical models. *Bulletin of the American Meteorological Society*, 88(1), 47–64.
- Erazo, B., Bourrel, L., Frappart, F., Chimborazo, O., Labat, D., Dominguez-Granda, L., Matamoros, D. and Mejia, R. (2018) Validation of satellite estimates (Tropical Rainfall Measuring Mission, TRMM) for rainfall variability over the pacific slope and coast of Ecuador. *Water*, 10(2), 213.
- Franchito, S.H., Rao, V.B., Vasques, A.C., Santo, C.M. and Conforte, J.C. (2009) Validation of TRMM precipitation radar monthly rainfall estimates over Brazil. *Journal of Geophysical Research: Atmospheres*, 114, D02105.
- Gourley, J.J., Hong, Y., Flamig, Z.L., Li, L. and Wang, J. (2010) Intercomparison of rainfall estimates from radar, satellite, gauge, and combinations for a season of record rainfall. *Journal of Applied Meteorology and Climatology*, 49(3), 437–452.
- Hamada, A., Murayama, Y. and Takayabu, Y.N. (2014) Regional characteristics of extreme rainfall extracted from TRMM PR measurements. *Journal of Climate*, 27(21), 8151–8169.
- Hirpa, F.A., Gebremichael, M. and Hopson, T. (2010) Evaluation of high-resolution satellite precipitation products over very complex terrain in Ethiopia. *Journal of Applied Meteorology and Climatology*, 49(5), 1044–1051.
- Hou, A.Y., Kakar, R.K., Neeck, S., Azarbarzin, A.A., Kummerow, C. D., Kojima, M., Oki, R., Nakamura, K. and Iguchi, T. (2014) The global precipitation measurement mission. *Bulletin of the American Meteorological Society*, 95(5), 701–722.
- Hu, Q., Yang, D., Li, Z., Mishra, A.K., Wang, Y. and Yang, H. (2014) Multi-scale evaluation of six high-resolution satellite monthly rainfall estimates over a humid region in China with dense rain gauges. *International Journal of Remote Sensing*, 35(4), 1272–1294.
- Huffman, G.J. (1997) Estimates of root-mean-square random error for finite samples of estimated precipitation. *Journal of Applied Meteorology*, 36(9), 1191–1201.
- Huffman, G.J. (2019) *The transition in multi-satellite products from TRMM to GPM (TMPA to IMERG)*. Greenbelt, USA: NASA, p. 1–5.
- Huffman, G.J., Adler, R.F., Arkin, P., Chang, A., Ferraro, R., Gruber, A., Janowiak, J., McNab, A., Rudolf, B. and Schneider, U. (1997) The global precipitation climatology project (GPCP) combined precipitation dataset. *Bulletin of the American Meteorological Society*, 78(1), 5–20.
- Huffman, G.J., Adler, R.F., Bolvin, D.T. and Nelkin, E.J. (2010) The TRMM multi-satellite precipitation analysis (TMPA). In: *Satellite Rainfall Applications for Surface Hydrology*. Dordrecht, Netherlands: Springer, pp. 3–22.
- Huffman, G.J. and Bolvin, D.T. (2015) *TRMM and Other Data Precipitation Data Set Documentation*. Greenbelt, USA: NASA. 1–44.
- Huffman, G.J., Bolvin, D.T., Nelkin, E.J., Wolff, D.B., Adler, R.F., Gu, G., Hong, Y., Bowman, K.P. and Stocker, E.F. (2007) The TRMM multisatellite precipitation analysis (TMPA): quasi-global, multiyear, combined-sensor precipitation estimates at fine scales. *Journal of Hydrometeorology*, 8(1), 38–55.
- Iguchi, T., Kozu, T., Meneghini, R., Awaka, J. and Okamoto, K. (2000) Rain-profiling algorithm for the TRMM precipitation radar. *Journal of Applied Meteorology*, 39(12), 2038–2052.
- Jaramillo, L., Poveda, G. and Mejía, J.F. (2017) Mesoscale convective systems and other precipitation features over the tropical Americas and surrounding seas as seen by TRMM. *International Journal of Climatology*, 37, 380–397.
- Jiang, H., Liu, C. and Zipser, E.J. (2011) A TRMM-based tropical cyclone cloud and precipitation feature database. *Journal of Applied Meteorology and Climatology*, 50(6), 1255–1274.
- Jiménez-Sánchez, G., Markowski, P.M., Jewtoukoff, V., Young, G.S. and Stensrud, D.J. (2019) The orinoco low-level jet: an investigation of its characteristics and evolution using the WRF model. *Journal of Geophysical Research: Atmospheres*, 124(20), 10696–10711.
- Joyce, R.J., Janowiak, J.E., Arkin, P.A. and Xie, P. (2004) CMORPH: a method that produces global precipitation estimates from passive microwave and infrared data at high spatial and temporal resolution. *Journal of Hydrometeorology*, 5(3), 487–503.
- Karaseva, M.O., Prakash, S. and Gairola, R. (2012) Validation of high-resolution TRMM-3B43 precipitation product using rain gauge measurements over Kyrgyzstan. *Theoretical and Applied Climatology*, 108(1–2), 147–157.
- Kidd, C., Bauer, P., Turk, J., Huffman, G., Joyce, R., Hsu, K.-L. and Braithwaite, D. (2012) Intercomparison of high-resolution precipitation products over Northwest Europe. *Journal of Hydro-meteorology*, 13(1), 67–83.
- Krakauer, N., Pradhanang, S., Lakhankar, T. and Jha, A. (2013) Evaluating satellite products for precipitation estimation in mountain regions: a case study for Nepal. *Remote Sensing*, 5(8), 4107–4123.
- Kummerow, C., Barnes, W., Kozu, T., Shiue, J. and Simpson, J. (1998) The Tropical Rainfall Measuring Mission (TRMM) sensor package. *Journal of Atmospheric and Oceanic Technology*, 15(3), 809–817.
- Kummerow, C., Simpson, J., Thiele, O., Barnes, W., Chang, A., Stocker, E., Adler, R., Hou, A., Kakar, R., Wentz, F., Ashcroft, P., Kozu, T., Hong, Y., Okamoto, K., Iguchi, T., Kuroiwa, H., Im, E., Haddad, Z., Huffman, G., Ferrier, B., Olson, W.S., Zipser, E., Smith, E.A., Wilheit, T.T., North, G., Krishnamurti, T. & Nakamura, K., et al. (2000) The status of the Tropical Rainfall Measuring Mission (TRMM) after two years in orbit. *Journal of Applied Meteorology*, 39(12), 1965–1982.

- Kurucz, M., Benczúr, A.A. and Csalogány, K. (2007) Methods for large scale SVD with missing values. In: *Proceedings of KDD Cup and Workshop*, Vol. 12. San José, USA: Citeseer, pp. 31–38.
- Lee, R.B., Barkstrom, B.R., Biting, H.C., Crommelynck, D.A.H., Paden, J., Pandey, D.K., Priestley, K.J., Smith, G.L., Thomas, S., Thornhill, K.L. and Wilson, R.S. (1998) Prelaunch calibrations of the clouds and the Earth's Radiant Energy System (CERES) tropical rainfall measuring mission and Earth Observing System morning (EOS-AM1) spacecraft thermistor bolometer sensors. *IEEE Transactions on Geoscience and Remote Sensing*, 36(4), 1173–1185.
- Levizzani, V., Amorati, R., and Meneguzzo, F. (2002). *A Review of Satellite-Based Rainfall Estimation methods*. Bologna, Italy: Consiglio Nazionale delle Ricerche, Istituto di Scienze dell'Atmosfera e del Clima, European Commission Project MUSIC Report (EVK1-CT-2000-00058), 66.
- Liu, Z., Ostrenga, D., Teng, W. and Kempler, S. (2012) Tropical Rainfall Measuring Mission (TRMM) precipitation data and services for research and applications. *Bulletin of the American Meteorological Society*, 93(9), 1317–1325.
- Maggioni, V., Meyers, P.C. and Robinson, M.D. (2016) A review of merged high-resolution satellite precipitation product accuracy during the Tropical Rainfall Measuring Mission (TRMM) era. *Journal of Hydrometeorology*, 17(4), 1101–1117.
- Mantas, V.M., Liu, Z., Caro, C. and Pereira, A. (2015) Validation of TRMM multi-satellite precipitation analysis (TMPA) products in the Peruvian Andes. *Atmospheric Research*, 163, 132–145.
- Marengo, J.A., Soares, W.R., Saulo, C. and Nicolini, M. (2004) Climatology of the low-level jet east of the Andes as derived from the NCEP–NCAR reanalyses: characteristics and temporal variability. *Journal of Climate*, 17(12), 2261–2280.
- Mätzler, C. and Standley A. (2000) Technical note: Relief effects for passive microwave remote sensing. *International Journal of Remote Sensing*, 21(12), 2403–2412.
- Mejía, J.F., Mesa, O., Poveda, G., Vélez, J., Hoyos, C., Mantilla, R., Barco, J., Cuartas, A., Montoya, M. and Botero, B. (1999) Distribución espacial y ciclos anual y semianual de la precipitación en Colombia. *DYNA*, 127, 7–24.
- Melo, D.C.D., Xavier, A.C., Bianchi, T., Oliveira, P.T., Scanlon, B. R., Lucas, M.C. and Wendland, E. (2015) Performance evaluation of rainfall estimates by TRMM multi-satellite precipitation analysis 3B42V6 and V7 over Brazil. *Journal of Geophysical Research: Atmospheres*, 120(18), 9426–9436.
- Meng, J., Li, L., Hao, Z., Wang, J. and Shao, Q. (2014) Suitability of TRMM satellite rainfall in driving a distributed hydrological model in the source region of Yellow River. *Journal of Hydrology*, 509, 320–332.
- Mohr, K.I., Slayback, D. and Yager, K. (2014) Characteristics of precipitation features and annual rainfall during the TRMM era in the Central Andes. *Journal of Climate*, 27(11), 3982–4001.
- Montoya, G.d.J., Pelkowski, J. and Eslava, J.A. (2001) Sobre los alisios del nordeste y la existencia de una corriente en el piedemonte oriental andino. *Revista de la Academia Colombiana de Ciencias Exactas, Físicas y Naturales*, 25(96), 363–371.
- Mourre, L., Condom, T., Junquas, C., Lebel, T., Sicart, J., Figueroa, R. and Cochachin, A. (2015) Spatio-temporal assessment of WRF, TRMM and in situ precipitation data in a tropical mountain environment (Cordillera Blanca, Peru). *Hydrology & Earth System Sciences Discussions*, 12(7), 6635–6681.
- Nair, S., Srinivasan, G. and Nemani, R. (2009) Evaluation of multi-satellite TRMM derived rainfall estimates over a western state of India. *Journal of the Meteorological Society of Japan Series II*, 87(6), 927–939.
- Nastos, P., Kapsomenakis, J. and Philandras, K. (2016) Evaluation of the TRMM 3B43 gridded precipitation estimates over Greece. *Atmospheric Research*, 169, 497–514.
- Negri, A.J., Xu, L. and Adler, R. (2002) A TRMM-calibrated infrared rainfall algorithm applied over Brazil. *Journal of Geophysical Research: Atmospheres*, 107(D20), LBA–15.
- Nesbitt, S.W., Zipser, E.J. and Cecil, D.J. (2000) A census of precipitation features in the tropics using TRMM: radar, ice scattering, and lightning observations. *Journal of Climate*, 13(23), 4087–4106.
- Nicholson, S.E., Some, B., McCollum, J., Nelkin, E., Klotter, D., Berte, Y., Diallo, B.M., Gaye, I., Kpabebe, G., Ndiaye, O., Noukpozoukou, J.N., Tanu, M.M., Thiam, A., Toure, A.A. and Traore, A.K. (2003) Validation of TRMM and other rainfall estimates with a high-density gauge dataset for West Africa. Part ii: validation of TRMM rainfall products. *Journal of Applied Meteorology*, 42(10), 1355–1368.
- North, G.R. and Nakamoto, S. (1989) Formalism for comparing rain estimation designs. *Journal of Atmospheric and Oceanic Technology*, 6(6), 985–992.
- Ochoa, A., Pineda, L., Crespo, P. and Willems, P. (2014) Evaluation of TRMM 3B42 precipitation estimates and WRF retrospective precipitation simulation over the Pacific–Andean region of Ecuador and Peru. *Hydrology and Earth System Sciences*, 18(8), 3179–3193.
- Overpeck, J.T., Meehl, G.A., Bony, S. and Easterling, D.R. (2011) Climate data challenges in the 21st century. *Science*, 331(6018), 700–702.
- Palomino-Ángel, S., Anaya-Acevedo, J.A. and Botero, B.A. (2019) Evaluation of 3B42V7 and IMERG daily-precipitation products for a very high-precipitation region in northwestern South America. *Atmospheric Research*, 217, 37–48.
- Petersen, W.A. and Rutledge, S.A. (2001) Regional variability in tropical convection: observations from TRMM. *Journal of Climate*, 14(17), 3566–3586.
- Poveda, G. (2004) La hidroclimatología de Colombia: una síntesis desde la escala inter-decadal hasta la escala diaria. *Revista de la Academia Colombiana de Ciencias*, 28(107), 201–222.
- Poveda, G., Alvarez, D.M. and Rueda, O.A. (2011) Hydro-climatic variability over the Andes of Colombia associated with ENSO: a review of climatic processes and their impact on one of the Earth's most important biodiversity hotspots. *Climate Dynamics*, 36(11–12), 2233–2249.
- Poveda, G., Jaramillo, A., Gil, M.M., Quiceno, N. and Mantilla, R.I. (2001) Seasonally in ENSO-related precipitation, river discharges, soil moisture, and vegetation index in Colombia. *Water Resources Research*, 37(8), 2169–2178.
- Poveda, G., Jaramillo, L. and Vallejo, L.F. (2014) Seasonal precipitation patterns along pathways of south American low-level jets and aerial rivers. *Water Resources Research*, 50(1), 98–118.
- Poveda, G. and Mesa, O.J. (1999) La corriente de chorro superficial del Oeste ('del Chocó') y otras dos corrientes de chorro en Colombia: climatología y variabilidad durante las fases del ENSO. *Revista Académica Colombiana de Ciencia*, 23(89), 517–528.



- Poveda, G. and Mesa, O.J. (2000) On the existence of Lloró (the rainiest locality on Earth): Enhanced ocean–land–atmosphere interaction by a low-level jet. *Geophysical Research Letters*, 27 (11), 1675–1678.
- Poveda, G., Vélez, J.I., Mesa, O.J., Cuartas, A., Barco, J., Mantilla, R.I., Mejía, J.F., Hoyos, C.D., Ramírez, J.M., Ceballos, L.I., Zuluaga, M.D., Arias, P.A., Botero, B.A., Montoya, M.I., Giraldo, J.D. and Quevedo, D.I. (2007) Linking long-term water balances and statistical scaling to estimate river flows along the drainage network of Colombia. *Journal of Hydrologic Engineering*, 12(1), 4–13.
- Poveda, G., Waylen, P.R. and Pulwarty, R.S. (2006) Annual and inter-annual variability of the present climate in northern South America and southern Mesoamerica. *Palaeogeography, Palaeoclimatology, Palaeoecology*, 234(1), 3–27.
- Rasmussen, K.L., Choi, S.L., Zuluaga, M.D. and Houze, R.A. (2013) TRMM precipitation bias in extreme storms in South America. *Geophysical Research Letters*, 40(13), 3457–3461.
- Rueda, O. and Poveda, G. (2006) Variabilidad espacial y temporal del chorro del ‘Chocó’ y su efecto en la hidroclimatología de la región del pacífico colombiano. *Meteorología Colombiana*, 10, 132–145.
- Sakamoto, M.S., Ambrizzi, T. and Poveda, G. (2011) Moisture sources and life cycle of convective systems over Western Colombia. *Advances in Meteorology*, 2011, 1–11.
- Sapiano, M.R., Janowiak, J.E., Shi, W., Higgins, R.W. and Silva, V.B. (2010) Regional evaluation through independent precipitation measurements: USA. In: *Satellite Rainfall Applications for Surface Hydrology*. Dordrecht, Netherlands: Springer, pp. 169–191.
- Satgé, F., Bonnet, M.-P., Gosset, M., Molina, J., Lima, W.H.Y., Zolá, R.P., Timouk, F. and Garnier, J. (2016) Assessment of satellite rainfall products over the Andean plateau. *Atmospheric Research*, 167, 1–14.
- Scheel, M., Rohrer, M., Huggel, C., Santos Villar, D., Silvestre, E. and Huffman, G. (2011) Evaluation of TRMM multi-satellite precipitation analysis (TMPA) performance in the Central Andes region and its dependency on spatial and temporal resolution. *Hydrology and Earth System Sciences*, 15(8), 2649–2663.
- Schneider, U., Becker, A., Finger, P., Meyer-Christoffer, A., Rudolf, B. and Ziese, M. (2011) *GPCC monitoring product version 4.0 at 1.0°: near real-time monthly land-surface precipitation from rain-gauges based on SYNOP and CLIMAT data*. Offenbach, Germany: Global Precipitation Climatology Centre. 10.5676/DWD\_GPCC/MP\_M\_V4\_100.
- Schneider, U., Becker, A., Finger, P., Meyer-Christoffer, A., Rudolf, B. & Ziese, M. (2011) *GPCC full data reanalysis version 6.0 at 1.0°: monthly land-surface precipitation from rain-gauges built on GTS-based and historic data*. Offenbach, Germany: Global Precipitation Climatology Centre. 10.5676/DWD\_GPCC/FD\_M\_V6\_100.
- Schneider, U., Becker, A., Finger, P., Meyer-Christoffer, A. and Ziese, M. (2018) *GPCC Full Data Monthly Product Version 2018 at 0.25°: Monthly Land-Surface Precipitation from Rain-Gauges Built on GTS-Based and Historical Data*. Offenbach, Germany: Global Precipitation Climatology Centre. 10.5676/DWD\_GPCC/FD\_M\_V2018\_025.
- Shin, K.-S. and North, G.R. (1988) Sampling error study for rainfall estimate by satellite using a stochastic model. *Journal of Applied Meteorology*, 27(11), 1218–1231.
- Skofronick-Jackson, G., Petersen, W.A., Berg, W., Kidd, C., Stocker, E.F., Kirschbaum, D.B., Kakar, R., Braun, S.A., Huffman, G.J., Iguchi, T., Kirstetter, P.E., Kummerow, C., Meneghini, R., Oki, R., Olson, W.S., Takayabu, Y.N., Furukawa, K. and Wilheit, T. (2017) The global precipitation measurement (GPM) mission for science and society. *Bulletin of the American Meteorological Society*, 98(8), 1679–1695.
- Stampoulis, D. and Anagnostou, E.N. (2012) Evaluation of global satellite rainfall products over continental Europe. *Journal of Hydrometeorology*, 13(2), 588–603.
- Su, F., Hong, Y. and Lettenmaier, D.P. (2008) Evaluation of TRMM multisatellite precipitation analysis (TMPA) and its utility in hydrologic prediction in the La Plata Basin. *Journal of Hydrometeorology*, 9(4), 622–640.
- Tapiador, F.J., Turk, F.J., Petersen, W., Hou, A.Y., García-Orteaga, E., Machado, L.A.T., Angelis, C.F., Salio, P., Kidd, C., Huffman, G.J. and de Castro, M. (2012) Global precipitation measurement: methods, datasets and applications. *Atmospheric Research*, 104, 70–97.
- Tian, Y. and Peters-Lidard, C.D. (2010) A global map of uncertainties in satellite-based precipitation measurements. *Geophysical Research Letters*, 37(24), L24407.
- Tian, Y., Peters-Lidard, C.D., Adler, R.F., Kubota, T. and Ushio, T. (2010) Evaluation of GSMaP precipitation estimates over the contiguous United States. *Journal of Hydrometeorology*, 11(2), 566–574.
- Tian, Y., Peters-Lidard, C.D., Eylander, J.B., Joyce, R.J., Huffman, G.J., Adler, R.F., Hsu, K.-I., Turk, F.J., Garcia, M. and Zeng, J. (2009) Component analysis of errors in satellite-based precipitation estimates. *Journal of Geophysical Research: Atmospheres*, 114, D24101.
- Torrealba, E.R. and Amador, J.A. (2010) La corriente en chorro de bajo nivel sobre los Llanos Venezolanos de Sur América. *Revista de Climatología*, 10, 1–20.
- Urrea, V., Ochoa, A. and Mesa, O.J. (2019) Seasonality of Rainfall in Colombia. *Water Resources Research*, 55(5), 4149–4162.
- Vera, C., Baez, J., Douglas, M., Emmanuel, C.B., Marengo, J., Meitin, J., Nicolini, M., Nogues-Paegle, J., Paegle, J., Penalba, O., Salio, P., Saulo, C., Silva Dias, M.A., Silva Dias, P. and Zipser, E. (2006) The South American low-level jet experiment. *Bulletin of the American Meteorological Society*, 87(1), 63–78.
- Wang, C. (2007) Variability of the Caribbean low-level jet and its relations to climate. *Climate Dynamics*, 29(4), 411–422.
- Ward, E., Buytaert, W., Peaver, L. and Wheeler, H. (2011) Evaluation of precipitation products over complex mountainous terrain: a water resources perspective. *Advances in Water Resources*, 34(10), 1222–1231.
- Wasserstein, R.L. and Lazar, N.A. (2016) The ASA’s statement on p-values: context, process, and purpose. *The American Statistician*, 70(2), 129–133.
- Yepes, J., Poveda, G., Mejía, J.F., Moreno, L. and Rueda, C. (2019) CHOCO-JEX: a research experiment focused on the CHOCO low-level jet over the far Eastern Pacific and Western Colombia. *Bulletin of the American Meteorological Society*, 100(5), 779–796.
- Yong, B., Ren, L.-L., Hong, Y., Wang, J.-H., Gourley, J.J., Jiang, S.-H., Chen, X. and Wang, W. (2010) Hydrologic evaluation of multi-satellite precipitation analysis standard precipitation products in basins beyond its inclined latitude band: a case study in Laohahe basin, China. *Water Resources Research*, 46(7), W07542.



- Zambrano-Bigiarini, M., Nauditt, A., Birkel, C., Verbist, K. and Ribbe, L. (2017) Temporal and spatial evaluation of satellite-based rainfall estimates across the complex topographical and climatic gradients of Chile. *Hydrology and Earth System Sciences*, 21(2), 1295–1320.
- Zipser, E.J., Cecil, D.J., Liu, C., Nesbitt, S.W. and Yorty, D.P. (2006) Where are the most intense thunderstorms on earth? *Bulletin of the American Meteorological Society*, 87(8), 1057–1072.
- Zulkafli, Z., Buytaert, W., Onof, C., Manz, B., Tarnavsky, E., Lavado, W. and Guyot, J.-L. (2014) A comparative performance analysis of TRMM 3B42 (TMPA) versions 6 and 7 for hydrological applications over Andean–Amazon river basins. *Journal of Hydrometeorology*, 15(2), 581–592.
- Zuluaga, M.D. and Houze, R.A., Jr. (2015) Extreme convection of the near-equatorial Americas, Africa, and adjoining oceans as seen by TRMM. *Monthly Weather Review*, 143(1), 298–316.

**How to cite this article:** Vallejo-Bernal SM, Urrea V, Bedoya-Soto JM, *et al.* Ground validation of TRMM 3B43 V7 precipitation estimates over Colombia. Part I: Monthly and seasonal timescales. *Int J Climatol.* 2020;1–24. <https://doi.org/10.1002/joc.6640>